Geomorphological signature of topographically controlled ice flow-switching at a glacier margin: Breiðamerkurjökull (Iceland) as a modern analogue for palaeo-ice sheets

LALLY, Amy, RUFFELL, Alastair, NEWTON, Andrew M.W., REA, Brice R, SPAGNOLO, Matteo, STORRAR, Robert D <http://orcid.org/0000-0003-4738-0082>, KAHLERT, Thorsten and GRAHAM, Conor

Geomorphology 454 (2024) 109184

Contents lists available at ScienceDirect

Geomorphology

journal homepage: www.journals.elsevier.com/geomorphology

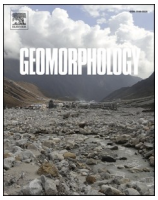

Geomorphological signature of topographically controlled ice flow-switching at a glacier margin: Breiðamerkurjökull (Iceland) as a modern analogue for palaeo-ice sheets

Amy Lally [a,*], Alastair Ruffell [a], Andrew M.W. Newton [a], Brice R. Rea [b], Matteo Spagnolo [b], Robert D. Storrar [c], Thorsten Kahlert [a], Conor Graham [a]

[a] School of Natural and Built Environment, Queen's University Belfast, University Road, Belfast BT7 1NN, UK
[b] School of Geosciences, University of Aberdeen, UK
[c] Department of the Natural and Built Environment, Sheffield Hallam University, Sheffield, UK

ARTICLE INFO

Keywords:
Glacial geomorphology
Ice marginal channels
Ice-flow switching
Iceland
Laurentide Ice Sheet
UAV

ABSTRACT

Ice low-switching, which can involve changes in ice flow velocity and direction, is crucial to a full understanding of ice masses and their response to climate change. A topographically controlled ice flow switch near a glacier margin was recently documented at Breiðamerkurjökull, southeast Iceland, where the central flow unit migrated eastward in response to variations in subglacial topography and the influence of Jökulsárlón glacial lagoon. This site provides an opportunity to study the geomorphic response to ice-margin reconfiguration. Investigating contemporary processes can offer valuable insights into analogous landforms created during the deglaciation of palaeo-ice sheets. The landform assemblage and topographic setting of our Icelandic study site is compared to a palaeo-example from Alberta, Canada, which was once covered by the Laurentide ice sheet.

Uncrewed aerial vehicle-(UAV) derived data was used to assess the geomorphic response to this switching and related processes across a 1.5 km^2 area of the central flow unit which deglaciated between 2010 and 2023. From 2010 to 2017, the landscape featured streamlined subglacial material, a stable subglacial esker system and proglacial lakes (Landsystem A), shifting to a spillway-dominated system between 2018 and 2023 (Landsystem B). Since 2018 this section of Breiðamerkurjökull has been retreating across a reverse slope bed, resulting in the formation of quasi-annual ice-marginal spillways. Meltwater impoundment at the ice margin, formed ice-contact lakes which eventually initiated ice-margin parallel spillways draining proglacial meltwater along the local land-surface gradient, towards Jökulsárlón. As the ice retreats, an ice-contact lake forms again at the new margin and initiates the erosion of the next ice-marginal spillway. The geomorphological signature demonstrates how subglacial topography and ice-flow switching can significantly influence ice and meltwater dynamics.

Since the glacier flow-switch, part of the central unit is now lake-terminating with areas of the margin evolving into a stagnant system, as it is now cut off from the accumulation centre. Therefore, Landsystem B could be analogous to regions of ice stream shut down and where ice masses retreated across reverse slope beds. For example, the Pakowki Lake region of Southeastern Alberta displays a similar landform assemblage and is presented as a palaeo-example in this work. Such insights are important for assessing the efficacy of numerical models in reconstructing the finer scale dynamics of past ice sheets during retreat.

1. Introduction

Understanding the behaviour of palaeo-ice sheets, particularly the ice streams that dominate ice sheet drainage (Bamber et al., 2000), is crucial for anticipating how modern ice sheets will respond to future climate forcing and internal processes/feedbacks. Flow-switching, characterised by changes in ice dynamics involving variations in velocity, direction, or both, has been observed in modern ice masses and inferred for palaeo ice sheets. (Anandakrishnan and Alley, 1997; Conway et al., 2002; Hulbe and Fahnestock, 2007; Ross et al., 2009; Stokes et al., 2009; Ó Cofaigh et al., 2010; Winsborrow et al., 2012).

Large-scale ice stream flow-switching can be triggered by multiple

* Corresponding author.
E-mail address: alally01@qub.ac.uk (A. Lally).

https://doi.org/10.1016/j.geomorph.2024.109184
Received 1 February 2024; Received in revised form 28 March 2024; Accepted 31 March 2024
Available online 3 April 2024

factors including: changes in sediment accumulation (Dowdeswell et al., 2006), basal thermal regime (Ó Cofaigh et al., 2010); rerouting of subglacial meltwater (water piracy) (Alley et al., 1994) and ice-divide migration (ice flow piracy) (Payne and Dongelmans, 1997; Greenwood and Clark, 2009; Brouard and Lajeunesse, 2019). Smaller scale, local (e.g. at a glacier/ice sheet margin) ice flow-switching is often related to subglacial topography (Storrar et al., 2017; Rice et al., 2024), because thinner ice has lower driving stress and is more susceptible to bed topography changes (Rice et al., 2024).

To improve model projections of future ice sheet behaviour, it is important to better understand complex processes influencing ice-margin and meltwater dynamics. Integral to improving ice sheet models is the use of reconstructed palaeo ice-sheet deglaciation patterns (e.g. Stokes et al., 2012; Young et al., 2020; Couette et al., 2023) to constrain/validate them. As ice sheets thin and retreat flow-switch mechanisms are likely to be important components of the deglacial dynamics (Brouard and Lajeunesse, 2019).

The glacial geomorphology of former ice-sheet beds can provide an opportunity for assessing flow-switching and landscape processes during deglaciation (e.g. Aylsworth and Shilts, 1989; Brennand and Shaw, 2011; Clark and Walder, 1994; Dewald et al., 2022; Evans et al., 2008; Gauthier et al., 2019; Newton and Huuse, 2017; Ojala et al., 2021; Stokes et al., 2009; Storrar et al., 2014). For example, meltwater landforms identify major meltwater routes which are typically assumed to form parallel to ice flow (Kleman and Borgström, 1996), meaning that orientation variations could provide evidence for changes in ice stream flow directions (Evans et al., 2020). Mapping spillways, which are meltwater-eroded gorges draining water from proglacial lakes, provides detail on deglaciation and palaeo-lake reconstructions (Jansson, 2003; Stokes and Clark, 2004; Slomka and Utting, 2018; Utting and Atkinson, 2019; Regnéll et al., 2023). The increased application of high-resolution DEMs across regions previously covered by ice sheets and glaciers provides opportunities to map and interpret complex landscapes (e.g. Delaney et al., 2018; Ahokangas et al., 2021; Dewald et al., 2021). They bridge the spatial resolution gap between field mapping and satellite imagery by allowing glacial landscapes to be examined at centimetre-scale resolution (Śledź et al., 2021). Repeat survey UAV derived DEMs are increasingly used in refining process-form models and landform identification (Evans et al., 2016b, 2023; Ely et al., 2017; Chandler et al., 2020a, 2020b; Lally et al., 2023; Śledź et al., 2023).

Icelandic glaciers, although not comparable in size to ice sheets, have provided useful analogues with which to develop landform-sediment-process associations, associated to ice sheet deglaciation (Price and Howarth, 1970; Eyles, 1983; Evans et al., 1999; Evans, 2011; Bennett and Evans, 2012; Storrar et al., 2015; Chandler et al., 2020a).

A glacier flow switch was documented at Breiðamerkurjökull, southeast Iceland, between 2006 and 2016 (Guðmundsson and Björnsson, 2016; Storrar et al., 2017) whereby the central flow unit migrated eastwards, controlled by the subglacial bed topography and the draw down effect of Jökulsárlón glacial lagoon (Fig. 1). The region of the flow switch described by Guðmundsson and Björnsson (2016) and Storrar et al. (2017) has now deglaciated, providing a unique opportunity to characterise the geomorphological signature connected to topographically controlled ice flow-switching that has been documented by remote sensing.

In this study, the glacial geomorphology of a 1.5 km^2 area, deglaciated between 2010 and 2023 and associated with the glacier flow-switch, is mapped three times (September 2021, May 2022 and May 2023) from UAV-derived data to investigate processes driving landscape evolution. A comparison is drawn between the Breiðamerkurjökull site and Pakowki Lake region in Southeast Alberta, a ~ 35,000 km^2 area once covered by the Laurentide ice sheet (LIS). In both locations it appears that subglacial topography exerted strong controls on ice-margin and meltwater dynamics.

2. Study areas

2.1. Breiðamerkurjökull setting and recent flow switch

Breiðamerkurjökull, a piedmont lobe outlet glacier of Vatnajökull ice cap in Southeast Iceland, comprises three major flow units: Mávabyggðarjökull (western flow unit), Esjufjallajökull (central flow unit), and Norðlingalægðarjökull (eastern flow unit) (Guðmundsson and Evans, 2022) (Fig. 1). The mean ice thickness of the Vatnajökull ice cap is 370 m which a max thickness of 950 m in 2010–2012 (Björnsson and Pálsson, 2020).

Breiðamerkurjökull is warm-based with average ice-margin temperatures of 0 °C in winter and 10 °C in summer (Björnsson and Pálsson, 2008). The glacier has an average mass balance of -0.6 ± 0.1 m w.e. a^{-1} per year (Guðmundsson et al., 2017). The glacier has retreated 4–7 km with 115 km^2 of the former subglacial bed has been deglaciated in the last 120 years (Guðmundsson et al., 2017).

The proglacial area features a ~ 1 m-thick till layer overlying up to 50 m of glaciofluvial sediments on fractured igneous bedrock (Boulton et al., 2007a). The south coast is characterised by a maritime climate, limited days below 0 °C prevents permafrost development (Etzelmüller et al., 2007), although frozen ground at Breiðamerkurjökull has been documented via the evolution of pitted sandar whereby glaciofluvial deposits the retreating ice margin (Price, 1971; Evans and Twigg, 2002; Guðmundsson and Evans, 2022). Geomorphological mapping from the mid-1900s to 2022 shows significant changes in the foreland due to rapid glacier downwasting and retreat (Howarth and Welch, 1969a, 1969b; Price, 1969, 1971, 1982; Price and Howarth, 1970; Evans and Twigg, 2000; Storrar et al., 2015; Guðmundsson and Evans, 2022; Lally et al., 2023) Proglacial meltwater accumulates at various ice marginal locations, leading to the formation and expansion of lakes like Jökulsárlón, the largest and deepest lake in Iceland (Guðmundsson et al., 2019)(. Jökulsárlón is a tidal lagoon as it is connected to the North Atlantic Ocean by a 70 m wide and ~ 6 m deep channel named Jökulsá (Brandon et al., 2017). The subglacial topography is characterised by an overdeepened trough extending up to 15 km upglacier of the eastern flow unit 2023 active margin, which will contribute to lake expansion with continued ice margin retreat (Björnsson, 1996).

Guðmundsson and Björnsson (2016) and Storrar et al. (2017) presented observations of a contemporaneous flow switch at Breiðamerkurjökull. This was evidenced by a lateral shift in the Esjufjallarönd medial moraine, separating the central and eastern flow units, by up to 900 m in the decade preceding 2016 (Guðmundsson and Björnsson, 2016). The moraine and part of the central flow unit was redirected towards Jökulsárlón from its previous land-terminating position (Storrar et al., 2017).

In 1945 the Esjufjallarönd moraine terminated in Jökulsárlón before transitioning to a land-terminating position from 1965 to 1998. In 2007, when the glacier was retreating over the deepest part of the Jökulsárlón trench (~ 300 m), transverse crevasses were formed indicating a change in flow direction by 45° east-southeast (Guðmundsson and Björnsson, 2016; Storrar et al., 2017). This change in flow direction initiated the formation of a recumbent fold in Esjufjallarönd during the 2010 melt season, with a total displacement of ~ 300 m by 2016.

The glacier flow-switch is thought to have been driven by the variations in subglacial topography across the central and eastern flow unit (Guðmundsson and Björnsson, 2016; Storrar et al., 2017). Velocities across Breiðamerkurjökull, which vary spatiotemporally, are influenced by ice thickness, subglacial sediments and topography (Baurley et al., 2020). Peak velocities increased from 1991 to 2015 but have since reduced due to decreased driving stress from surface slope changes as the glacier thins. Velocities are greatest in the eastern flow unit due to the expansion of Jökulsárlón, impacting ice-surface slope and driving stresses (Guðmundsson and Björnsson, 2016; Baurley et al., 2020). Surface lowering, notably over the deepest parts of the trench, increasing velocity and drawdown of ice, are accelerating the margin

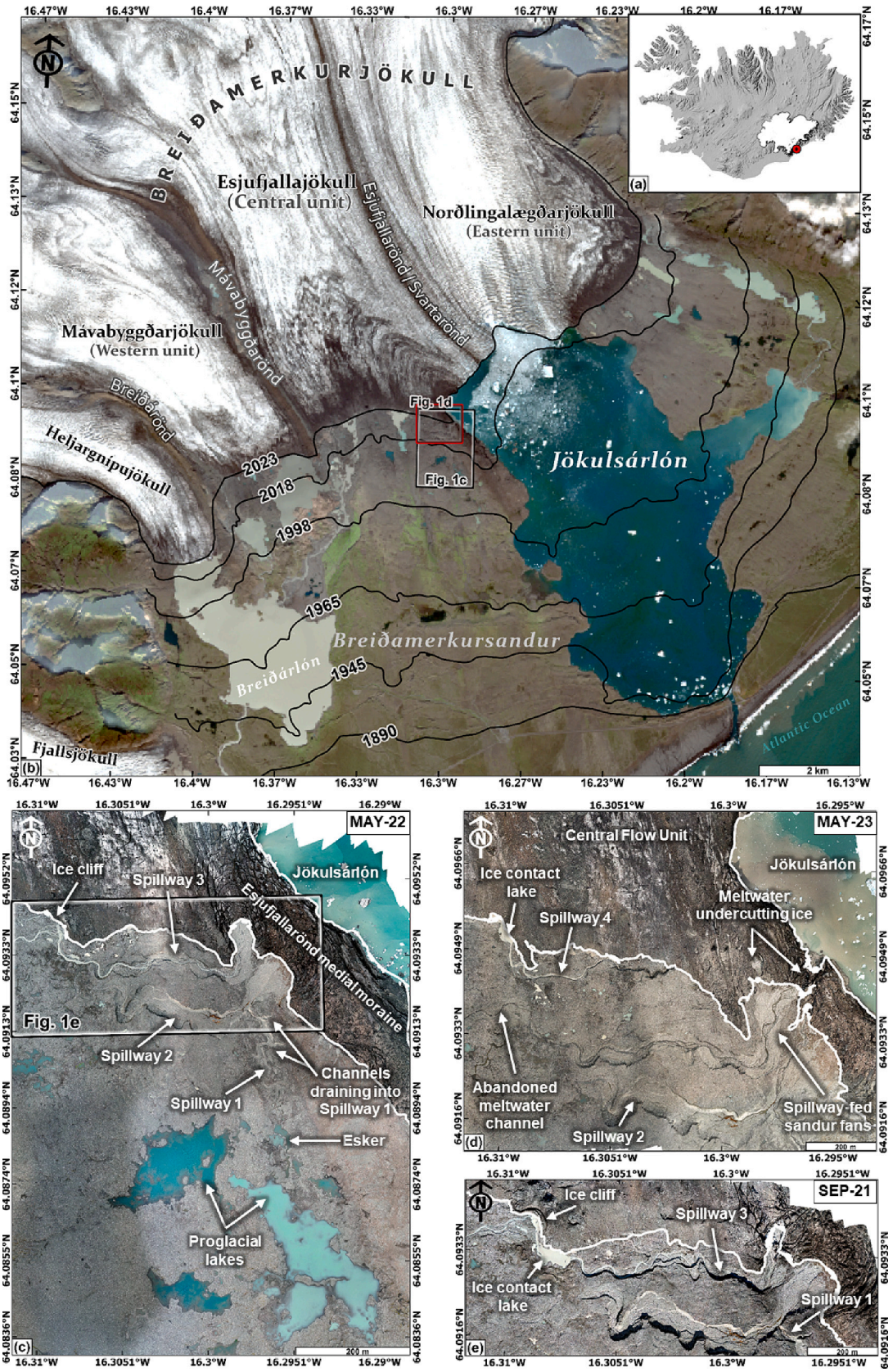

Fig. 1. a) red dot indicating Breiðamerkurjökull location on the south side of the Vatnajökull ice cap (Copernicus EU-DEM); b) Breiðamerkurjökull and associated foreland with Fig. 1c and 1e extents (basemap Sentinel-2 True Colour 15/09/2023); c-e) UAV-derived orthomosaics produced of geomorphology map extents for the three study periods: September 2021 (e), May 2022 (c) and May 2023 (d). Active ice margins are delineated in white.

retreat (Voytenko et al., 2015).

The presence of Breiðárlón proglacial lake at the ice-margin of Heljargnipukjökull (Fig. 1), the most westerly flow unit, does not appear to have impacted ice flow of the adjacent flow unit and the velocity of this flow unit has remained constant since 1991 (Baurley et al., 2020). Breiðárlón is shallow (~ 40 m) and sits above sea level, unlike Jökulsárlón which is much deeper and extends below sea level (Guðmundsson et al., 2017) Water depth has been identified as a controlling factor for flow switches in fjord systems (Briner et al., 2009), marine-terminating glaciers (Stokes et al., 2014) and potentially palaeo-ice streams (Briner et al., 2020).

Since the flow-switch, satellite image observations identified the formation of ice-marginal channels (perpendicular to ice flow) at Esjufjallajökull (Fig. 1c-e) which have also been identified in palaeo-glacial settings (e.g. Greenwood et al., 2007; Atkinson et al., 2014; Utting and Atkinson, 2019; Gauthier et al., 2022). The land-terminating section of the central flow unit is no longer part of the active ice flow which now preferentially flows towards the eastern flow unit and Jökulsárlón. This now stagnant ice margin could provide a modern analogue for areas of palaeo-ice margin reconfiguration.

2.2. The Pakowki Lake region (Southeast Alberta, Canada) glacial setting

The use of modern analogues, such as Breiðamerkurjökull, can provide support for palaeo-ice sheet reconstructions (Evans et al., 1999). It has been suggested that Breiðamerkurjökull is a good analogue to soft-bedded areas of the Laurentide Ice Sheet (LIS) (Evans et al., 1999; Boulton et al., 2007a) and as the glacier continues to thin and retreat, the bed topography may exert greater control on ice dynamics, providing modern analogues for different regions of ancient deglaciated landscapes.

Southern Alberta is characterised by a land-terminating ice-stream margin landsystem (Evans et al., 2014). This region was once covered by the LIS where it was underlain by a deformable bed of unconsolidated sediments and was likely characterised by a thin low gradient ice margin which was thus susceptible to topographically directed flow direction changes (Evans et al., 1999). Evans et al. (1999) noted the independent behaviour of different ice streams, whereby each flow unit behaved differently depending on ice thickness, flow unit size, width, ice margin type, ice piracy and subglacial topography.

In the Pakowki Lake region, which sits southwest of the Cyprus Hills, drainage is dominated by northeasterly flow into Hudson Bay and the Beaufort Sea (Beaney and Shaw, 2000) (Fig. 2a) and the Pakowki Lake depression, northwest of the preglacial drainage divide, occupies the lowest elevation in the region (Fig. 2b).

Previous work has mapped the glacial geomorphology and landforms in the area (e.g. Westgate, 1968; Shetsen, 1987; Kulig, 1996; Beaney and Shaw, 2000; Beaney, 2002; Evans et al., 2008, 2012, 2014; Atkinson et al., 2018), which are consistent with a lobate ice margin (Evans et al., 2014). The glacial geomorphology mapped by Atkinson et al. (2018) shows ribbed moraines over Cretaceous bedrock with superimposed curved recessional moraines (Fig. 2c). Ice-marginal channels were formed by meltwater flow along the ice margin due to the proglacial topography, which dips towards the palaeo-ice margin (Westgate, 1968). The main ice-marginal channels include the Etzikom and Chin Spillways which are both over 1 km wide and up to 75 m deep (Christiansen, 1977). Further incision of these channels during the Holocene is negligible due to the semi-arid climate in the region (Beaney, 2002). Ice-contact palaeo-lakes, Lake Lethbridge and Lake Taber, drained through these overflow outlets following the regional gradient (Evans, 2000; Evans et al., 2014; Utting and Atkinson, 2019). Pakowki lake sediments are estimated to be ~14.5 ka BP (Westgate, 1968) which is consistent with palaeo-ice margin extent associated with the Chin Spillway 14.5–14 ka BP (Dalton et al., 2020) (Fig. 2b).

3. Methods

3.1. Terminus, moraine, and sediment plume mapping

The glacier terminus, Esjufjallarönd and Mávabyggðarönd medial moraine locations from 1985 to 2023 were digitised in ArcGIS Pro v3.1.1. using a combination of Landsat, Sentinel-2, RapidEye and Planetscope satellite imagery. The margins and moraines were mapped monthly between April and October, excluding periods of dense cloud cover. Sediment plumes entering Jökulsárlón were mapped as point features from Sentinel-2 imagery for 2017–2023 to identify locations of subglacial meltwater outlets along the lake-terminating section of the central flow unit.

3.2. UAV data collection and processing

The study area (Fig. 1 c-e) was surveyed using a DJI Phantom 4 RTK quadcopter UAV three times: 5–10 September 2021, 6–12 May 2022 and 13–16 May 2023. Adverse weather conditions prevented UAV data collection during an additional survey season (5–8 September 2022) when only ground-based observations were possible. Agisoft Metashape v1.8.1. was used to process imagery following a structure-from-motion photogrammetry with multi-view stereopsis workflow (Westoby et al., 2012). Data were collected in RTK (real-time kinematics) mode, which have a position accuracy of ~ 0.015 m. The orthomosaics and digital elevation models (DEMs) have a horizontal resolution of 6 cm. The Scientific Colour Map Batlow was used for the visualisation of DEMs to prevent visual distortion (Crameri, 2020).

3.3. Geomorphological mapping

Landforms were digitised in ArcGIS Pro at 1:200 scale by analysing a combination of data: orthomosaics, DEMs, slope-gradient models, and traditional (Azimuth.

315° and 45°) and multi-directional oblique weighted Hillshades. All available cloud-free satellite imagery across the study site was assessed during the digitisation and map interpretation process. This included a combination of Planet, Sentinel-2 satellite and Landsat (4TM, 5TM and 8OLI) images. Field mapping and verification was undertaken over three field campaigns: 6–12 May 2022, 5–8 September 2022 and 13–16 May 2023, following procedures outlined by Chandler et al. (2018). The extent of each of the geomorphology maps is presented in Fig. 1c-e. A colour palette consistent with the existing Breiðamerkurjökull geomorphology map time-series was used where possible (e.g. orange for fluted till, yellow for glaciofluvial deposits) (Howarth and Welch, 1969a;Howarth and Welch, 1969b; Evans and Twigg, 2000; Guðmundsson and Evans, 2022). The Breiðamerkurjökull study area was compared to the Pakowki Lake region using the Alberta Sustainable Resources Development 25 m Provincial DEM (available from https://open.alberta.ca/) and the Alberta glacial landforms dataset (Atkinson et al., 2018).

4. Results

4.1. Medial moraine positions 1985–2023

The Esjufjallarönd moraine was land terminating in 1985 with a straight NW-SE trajectory (Fig. 3c). In 2007, as the eastern flow unit was retreating over the deepest part of Jökulsárlón (Fig. 3b), the moraine shifted eastward by ~ 80 m; by 2010 it had shifted another 85 m. A recumbent fold in the medial moraine was initiated in 2012, becoming prominent by 2015. By 2016, the moraine was displaced by ~ 300 m. The fold hinge at the ice margin (Fig. 3f) was eroded between May and June 2017, diverting the medial moraine into Jökulsárlón (Fig. 3d). Since 2017, it has continued to terminate in the glacial lagoon with a total lateral migration of ~ 750 m occurring between 1985 and 2023.

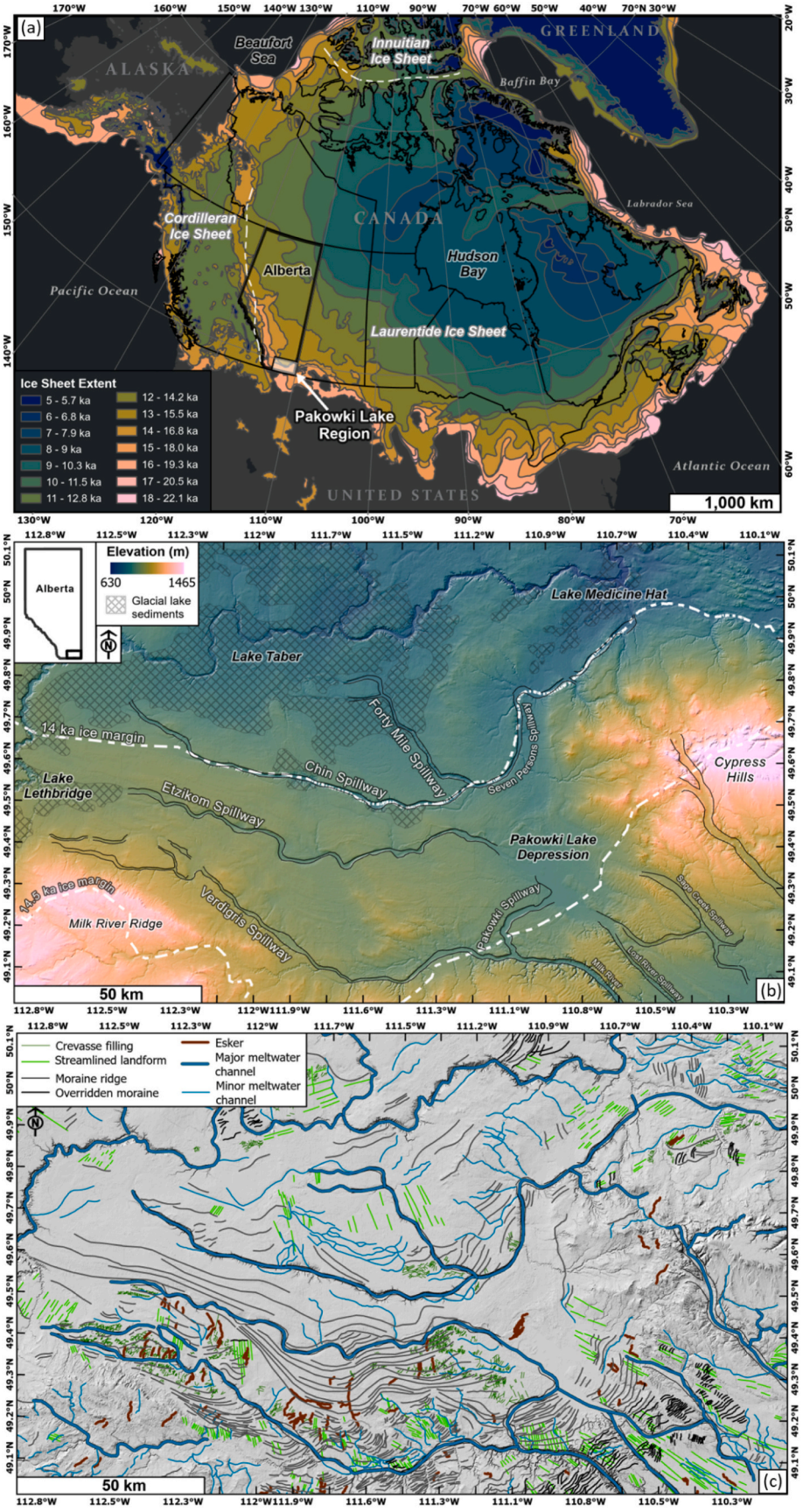

(caption on next page)

Fig. 2. a) Former ice sheet margins for the North American Ice Sheet Complex from Dalton et al. (2020) with the study area in Southeast Alberta highlighted (ESRI basemap), b) Pakowki Lake region in Southeastern Alberta (25 m DEM overlain onto a hillshade) with locations of meltwater eroded spillways, subglacial lake sediments (Evans et al., 2012) and former ice-margins (Dalton et al., 2020) and c) Glacial geomorphology of the region mapped by Atkinson et al. (2014, 2018) overlain on a Hillshade.

During May and June 2023, meltwater channels cut through the ice leaving a 1 km long ice-cored moraine section detached from the active margin extending 1 km south into the foreland (Fig. 3g). Contrastingly, the trajectory of the Mávabyggðarönd medial moraine along the western margin of the central flow unit has remained constant throughout the study period (Fig. 3c).

4.2. Glacial geomorphology

Fig. 4 shows the mapped features and landforms, while Fig. 5 provides glacial geomorphology maps for each of the three study periods: September 2021, May 2022 and May 2023. The extents of the geomorphology maps are presented in Fig. 1 c-e.

Ice and ice-cored moraines were mapped as a single feature, as it was difficult to confidently separate the debris rich glacier margin from the Esjufjallarönd medial moraine. The foreland is primarily composed of unconsolidated sands and gravels, most of which were streamlined and closely associated with flutings, elongated, in the direction of ice flow, low relief ridges (< 0.5 m), and geometric (< 0.5 m) low relief ridges, representing previous ice fracture/basal crevasse locations. Streamlined areas, and those containing crevasse-squeeze ridges and flutings, were classified as streamlined subglacial material or ground moraine (Guðmundsson and Evans, 2022). The region once covered by the Esjufjallarönd medial moraine contains a rubble veneer. Individual boulders were not mapped.

Flutings trend N-S, except for those uncovered post 2021 which trend NNW-SSE. Geometric ridge networks are concentrated on the eastern side of the May 2022 glacial geomorphology map, an area once covered by the Esjufjallarönd medial moraine. These ridges are predominantly perpendicular to ice flow and flutings, although there are clusters of randomly orientated ridges. Downwasting and retreat of snout ice, west of the spillway-fed sandur fans, between May 2022 and May 2023 revealed a ~ 1125 m^2 area of densely spaced, every 1–5 m, ridges.

This cluster of ridges are almost all NNE-SSW trending. The geometric ridges have been interpreted as crevasse-squeeze ridges forming in deformable substrate beneath heavily fractured, stagnant and rapidly downwasting snout ice (Rea and Evans, 2011; Evans et al., 2016a).

Glaciofluvial deposits, both erosional and depositional in origin, include flat sand/gravel outwash fans, linear sandar, spillways and gorges. Abandoned channels form either a braided pattern in lower gradient glaciofluvial outwash areas or isolated channels in higher gradient areas.

Eskers were delineated based on change of elevation and morphology. A 560 m long NW-SE trending esker emerged from the ice between 2014 and 2017 (Fig. 6). The esker crest height remained constant indicating a subglacial origin, and the landform resides in a depression associated with hummocky topography and proglacial lakes. Esker enlargements were included in the footprint. These are areas of the esker ridge that are significantly wider, up to 32 m, than the main ridge, up to 10 m in width, and provides evidence for subglacial conduit collapse (Dewald et al., 2021). Eskers uncovered between 2022 and 2023 (Fig. 5c) are orientated in multiple directions and are <1.5 m high, 25 m long and 4 m in width.

Hummocky meltwater tracts, represented by irregular mounded terrain, are usually found in transition areas between streamlined subglacial and glaciofluvial deposits. Satellite image analysis indicates after deglaciation most of these areas were initially covered by proglacial meltwater. Although some minor terracing was noted along the flanks of the esker, glaciolacustrine deposits were not differentiated from the hummocky terrain left behind as ponded proglacial meltwater dried up/drained away over time.

Proglacial water features include proglacial lakes, channels and water filled depressions. The underlying geomorphology of these areas is unknown. Proglacial lakes dominate in the region uncovered from 2010 to 2017. In 2021–2023, meltwater primarily pooled at the ice-margin and flowed west to east through meltwater-eroded spillways or gorges. The meltwater then flowed across spillway-fed sandur fans and back under the active ice-margin (2021−2022) and into Jökulsárlón glacial lagoon (2023).

4.3. Spillway evolution and sediment plumes

Terminus locations, cross and along flow elevation profiles over the 2022 study area indicate that from 2018 onwards, the emerging topography dips northeast so that the glacier is retreating across a retrograde bed (Fig. 6 Profile A-E). There are four large meltwater eroded spillways in the study area, Spillways 1–4. On the eastern side of Spillway 1, a 12000m^2 ice-dammed water body drained between May and June 2019, with a 4000 m^2 lake draining from the western side between 28th of June and 1st of July in the same year. This ice flow parallel spillway remained partially covered by ice/ice-cored moraine until August 2020.

During the 2018 ablation season, meltwater flowing from west to east, ponded against and undercut the ice-margin. Ice blocks broke off from this ice-margin forming an ice cliff (Fig. 6). The drainage of a 15,000 m^2 ice-contact lake in July 2019 formed Spillway 2, which remained active throughout 2020 and formed ~W-E (i.e. perpendicular to ice flow). Additional to these ice-contact lake drainage events, an embayment in the lake terminating ice margin of the central flow unit, where it entered Jökulsárlón formed between 9th and 27th of May 2019 (Fig. 3e). Surface gradient changes associated with its formation directed drainage into the embayment evidenced by a concentration of sediment plumes.

As the ice retreated during 2020–2021, meltwater began pooling at the new margin. Between 21st and 22nd of May 2021, Spillway 3 initiated following the drainage of a 97,000 km^2 ice contact lake which generated sediment plumes in the embayment. Meltwater drained from west to east through Spillway 3 during the 2021 meltwater season. Spillway 3 still contained a shallow (< 30 cm) active channel during the May 2023 field campaign which drained water from the detached ice block north of the channel initiation site (Fig. 5c).

In June 2022 sediment plumes in Jökulsárlón emanating from the end of Spillway 3, represent a proglacial sediment source. Additional plumes were observed 150 m west of the 2021 plume locations, likely representing sediment release from a subglacial source. In April 2023 sediment plumes were observed 50 m north of the Spillway 3 terminus in Jökulsárlón, coinciding with the initiation of Spillway 4 between April and May 2023. By June 7th, 2023, satellite imagery shows that Spillway 4 is abandoned and no longer connected to the ice-contact lake at the retreating ice-margin.

Between May 16th and August 17th 2023, the remaining ice-cored moraine separating Jökulsárlón from the central flow unit foreland had collapsed in response to meltwater undercutting the ice. Sediment plumes continued to emanate from the same location throughout the 2023 ablation season, perhaps indicating a new spillway location or a stable subglacial meltwater supply (Fig. 3e).

4.4. Comparison to Pakowki Lake Region

Fig. 7 presents topographic and geomorphological comparisons

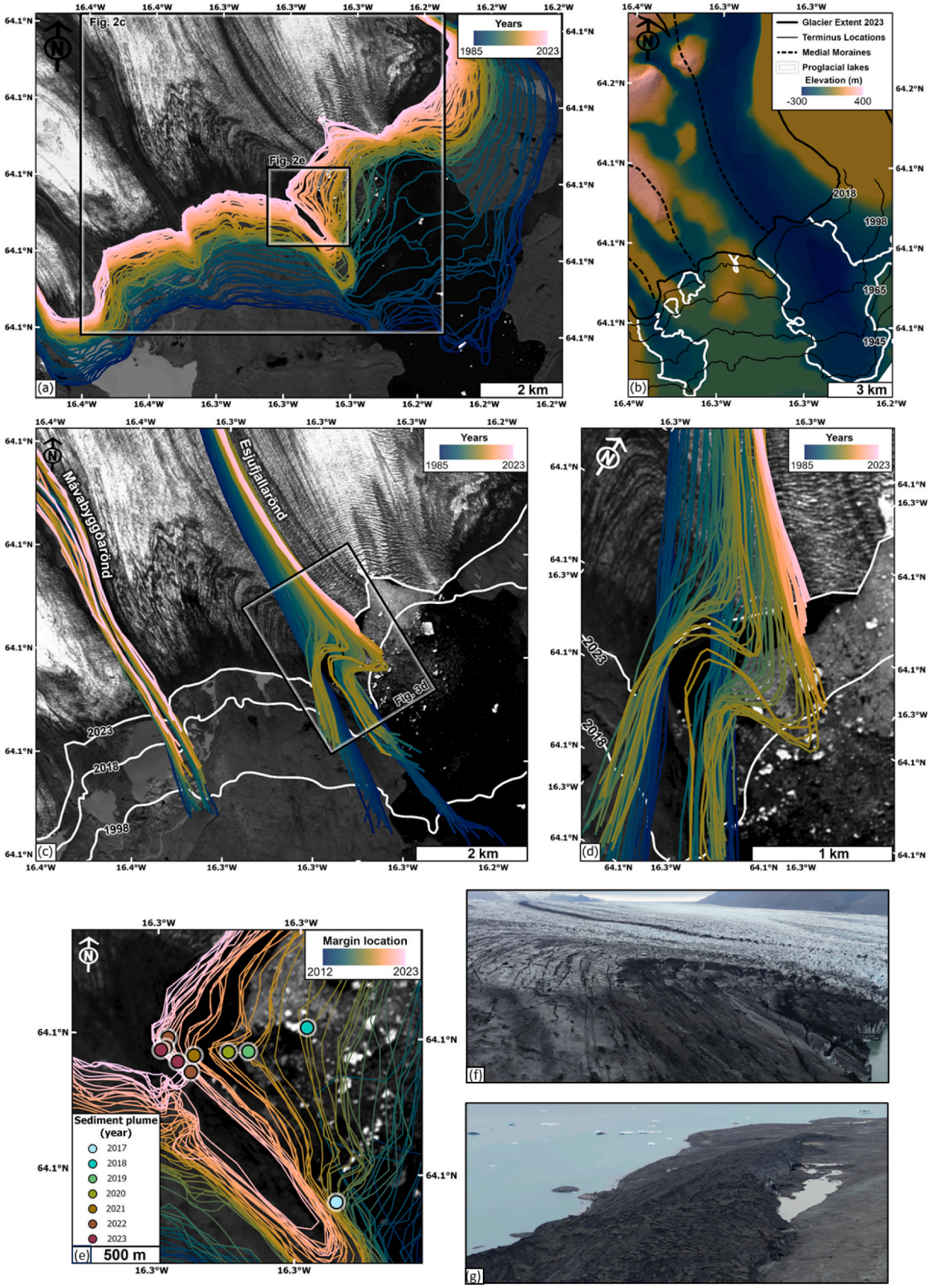

Fig. 3. a) Terminus locations of Breiðamerkurjökull from 1985 to September 2023; b) Subglacial topography digitised from contours provided from radio-echo sounding data (Bjornsson, 1996); c) Mávabyggðaröndd and Esjufjallaröndd medial moraine locations 1985–2023; d) zoomed in area of Esjufjallaröndd medial moraine locations; e) selection of sediment plume locations entering Jökulsárlón from 2017 to 2023 (basemaps 15/09/2023 Sentinel-2 satellite image); f) September 2022 UAV photo of the folded moraine, with the redirected moraine in the distance (photo facing northeast); g) September 2022 UAV photo of the ice-cored Esjufjallaröndd medial moraine extending 1 km south of the active ice margin, with Jökulsárlón on the left and the central flow unit foreland on the right (photo facing south).

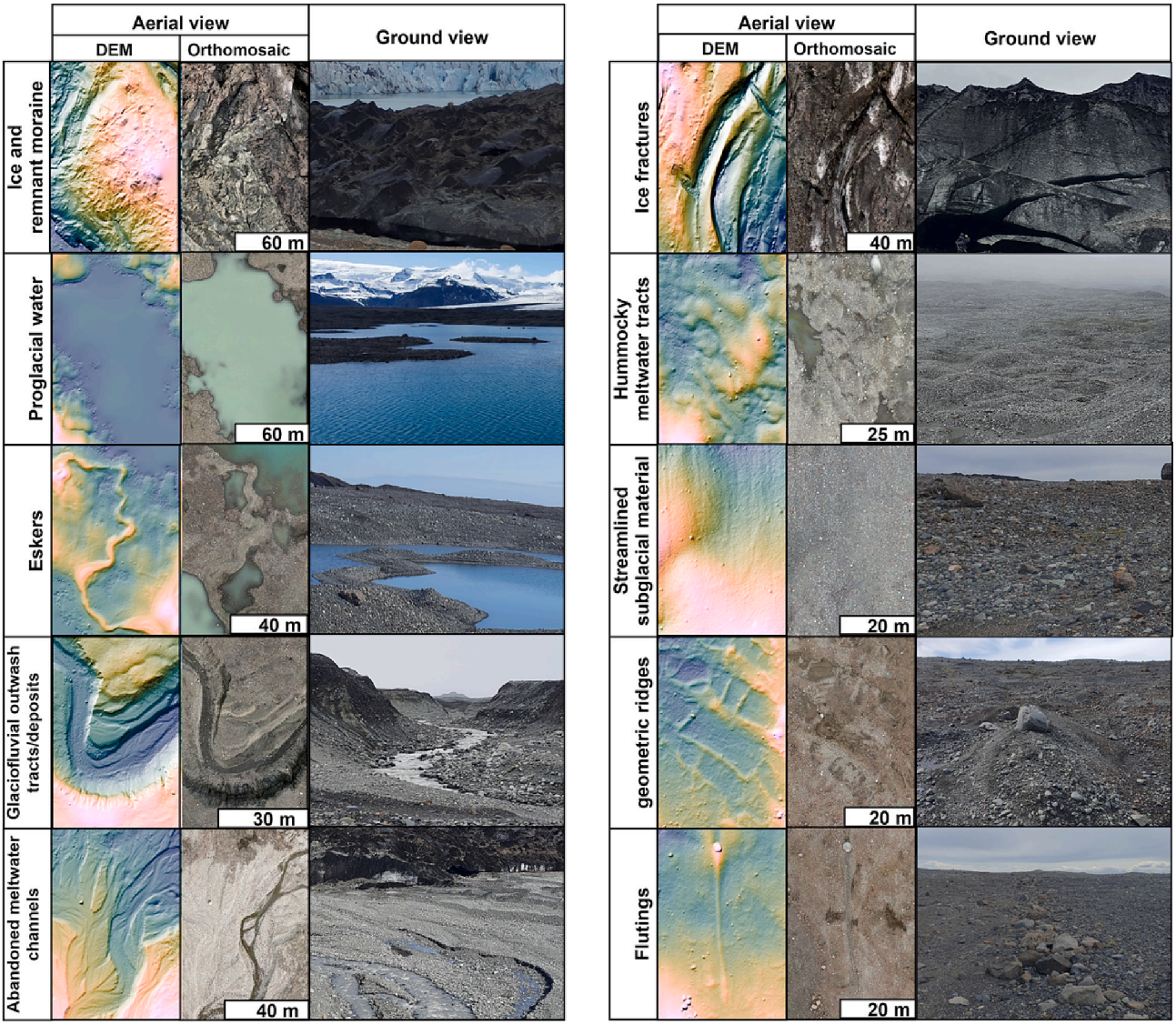

Fig. 4. Aerial view of the mapped features (DEM) with an example of the ground view from field photos. The DEM is underlain by an azimuth 315° Hillshade, dynamic range activated so each DEM elevation ranges from lowest (blue), intermediate (green/yellow) to highest (pink).

between the Breiðamerkurjökull study area and the Pakowki Lake region, Southeastern Alberta. Across and along flow elevation profiles (Fig. 7, profiles A and B) show the former subglacial bed dipping northeast (back towards the retreating ice margin) in both locations.

The Pakowki Spillway dips towards the lake depression and palaeo-ice margin, like Spillway 1 at Breiðamerkurjökull (Fig. 7 Profile C). Hummocky meltwater tracts appear on either side of both the Pakowki Spillway and Spillway 1 (Fig. 7g-h), which is not observed between the ice-margin parallel spillways (2–4).

Elevation profiles for the Pakowki Lake ice-margin parallel spillways (the Chin and Etzikom spillways) dip eastwards towards the lake depression, in a similar fashion to Spillways 2 and 3 at Breiðamerkurjökull (Fig. 7 profiles D and E). Further similarities between these sets of spillways include their parallel relationship and terracing along the channel. Entering Pakowki Lake from the west, the Etzikom Spillway was initiated at higher elevations and ends in a glaciofluvial outwash fan in the Pakowki Lake depression, similar to Spillway 2 at Breiðamerkurjökull. The Chin Spillway sits ~ 20 km north of the Etzikom Spillway, with a palaeo-flow direction of west to east and then diverted to the north which is also seen in the orientation of Spillway 3 at Breiðamerkurjökull.

Similar landforms are observed in the interfluve sections of these spillways which include thin channels draining into the spillways (e.g. 14 m deep and 320 m wide Fig. 7a and < 0.5 m deep and 2 m wide Fig. 7b) and short low relief eskers with a meander (e.g. 18 m high Fig. 7c and < 0.5 m high at Fig. 7d). A spillway-fed sandur fan lies at the downslope end of the Etizkom Spillway, where the sand and gravels with cut and fill structure indicate deposition in shallow water (Westgate, 1968), which is consistent with the braided outwash fan at Spillway 2 at Breiðamerkurjökull (Fig. 7c-d).

Northeast of the Chin Spillway, the Forty Mile Spillway connects to the Chin Spillway and flows northeast in the Seven Persons Spillway. Spillways 3 and 4 at Breiðamerkurjökull may meet when draining into Jökulsárlón, in a comparable manner to Forty Mile and Chin spillways.

5. Interpretation and discussion

5.1. Geomorphological evolution in response to glacier-flow switching and subglacial topography

The geomorphology maps presented in Fig. 5 show that when the glacier was retreating across a flat bed, the landform assemblage was

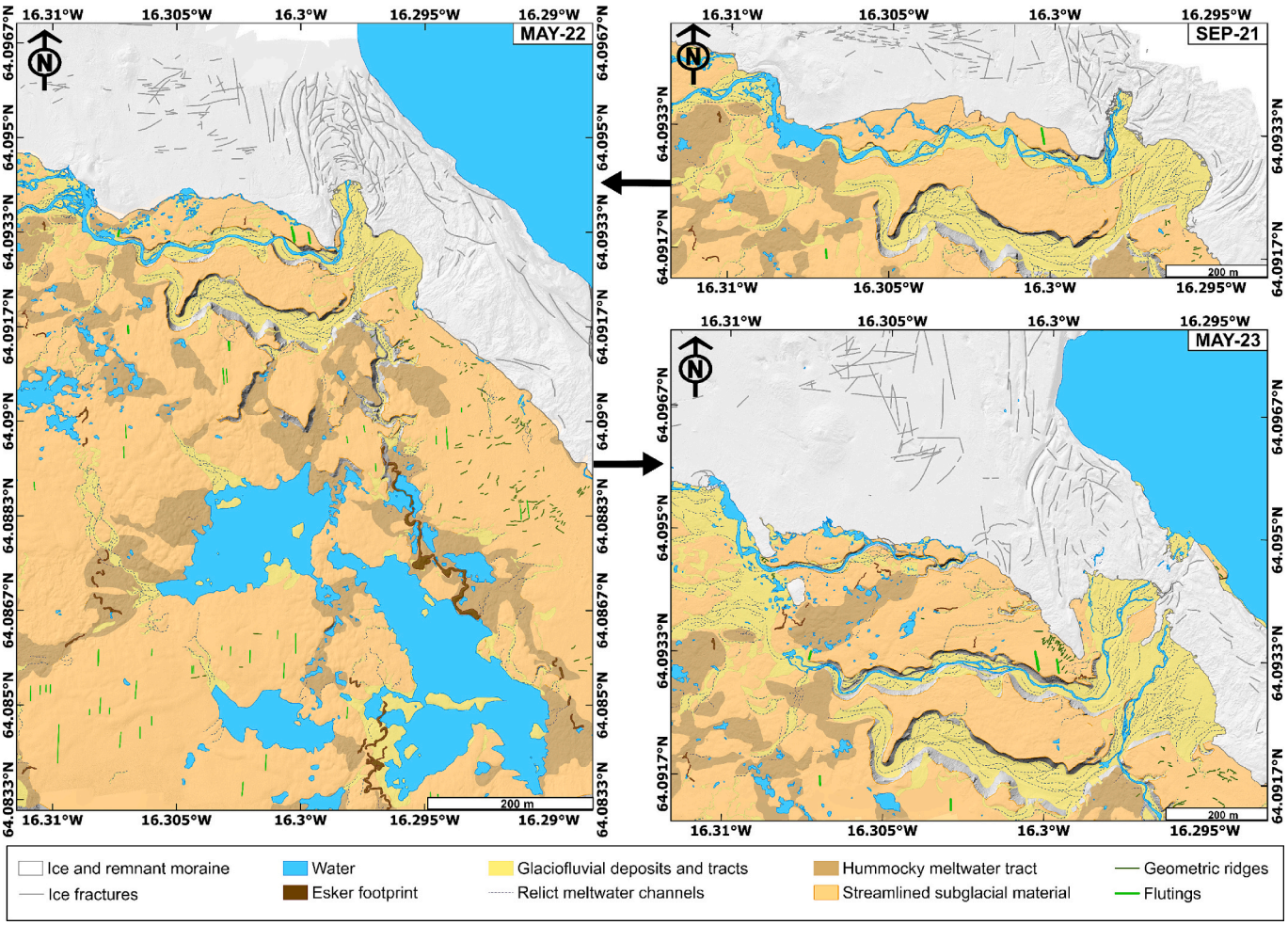

Fig. 5. Time-series of geomorphology maps depicting the ice-marginal environment of the central flow unit (see Fig. 1c-e for orthomosaics and extents of each map area): a) entire study area in May 2022 (1:6500 scale when printed on A3 paper), the ice margin in b) September 2021 (1:5000 scale) and c) May 2023 (1:5000 scale).

dominated by streamlined subglacial sediments, stable esker systems, hummocky meltwater tracts and proglacial lakes. This assemblage, representative of the landscape uncovered between 2010 and 2017, is termed "Landsystem A" (Fig. 8a).

The presence of long eskers flanked by water-filled depressions provide evidence for a subglacial drainage route, aligning with the temperate glacier landsystem (Evans and Twigg, 2002). The straight trajectory and length (> 500 m) of the solitary esker uncovered between 2014 and 2017 (Fig. 9a) indicates deposition in a stable subglacial channel (Price, 1969; Boulton et al., 2007b). Furthermore, the ridge morphology remained constant throughout the study period with no surface lowering observed, unlike englacial esker evolution at other areas of the Breiðamerkurjökull margin (Lally et al., 2023). The esker positions are also consistent with the location and trajectory of meltwater portal 8 presented by Boulton et al. (2007a). Along with groundwater control (Boulton et al., 2007b), the location of this esker is consistent with a medial moraine location which can supply both sediment and water to the channel (Storrar et al., 2015).

Since 2018 the glacier has retreated across a reverse slope bed (Fig. 9d) and part of the central flow unit is now lake-terminating due to the flow switch (Fig. 9c). Since then, the landform assemblage has become dominated by ice-margin parallel spillways forming quasi-annually from 2019 to 2023 (Fig. 9b) due to ice retreat, local topography and impoundment of water at the ice margin. This landform assemblage is termed "Landsystem B" (Fig. 8b). Once the channels were initiated, they deepened via erosion of the ice-proximal side of the slope. Proglacial water from the west of the study area was directed eastwards through these spillways eventually draining into Jökulsárlón. The small, fragmented eskers uncovered from 2018 onwards, likely represent glaciofluvial deposition in transient subglacial channels formed during a single meltwater season rather than recording the locations of stable subglacial meltwater drainage over multiple years.

The subglacial bed near the Mávabyggðarjökull medial moraine side of the central flow unit is also overdeepened (Fig. 3b) but the glacial geomorphology is different to the eastern study site. The foreland associated with Mávabyggðarönd medial moraine is characterised by buried ice with kame and kettle topography (Guðmundsson and Evans, 2022). As meltwater is often concentrated along medial moraine locations (Storrar et al., 2015), the diversion of the Esjufjallarönd moraine may have been accompanied by a diversion in the established meltwater system, which previously deposited the long esker in Landsystem A. The lack of a major meltwater supply would prevent snout burial by glaciofluvial outwash deposition. Subglacial hydraulic modelling by Storrar et al. (2017) corroborates that meltwater preferentially flows into the Jökulsárlón trench (Fig. 3b). This is supported by the time-series geomorphology maps (Fig. 5), illustrating meltwater flowing along the local gradient with all ice-marginal and proglacial meltwater draining under the ice/moraine into Jökulsárlón (Fig. 9c).

The spillways mapped at Breiðamerkurjökull, are eroded into streamlined subglacial material. The preservation of ice-flow direction indicators, such as flutings, at a warm-based glacier suggests water reaching the bed did not have sufficient energy or duration to destroy these landforms. This provides further evidence for the diversion of meltwater and main subglacial channels into Jökulsárlón.

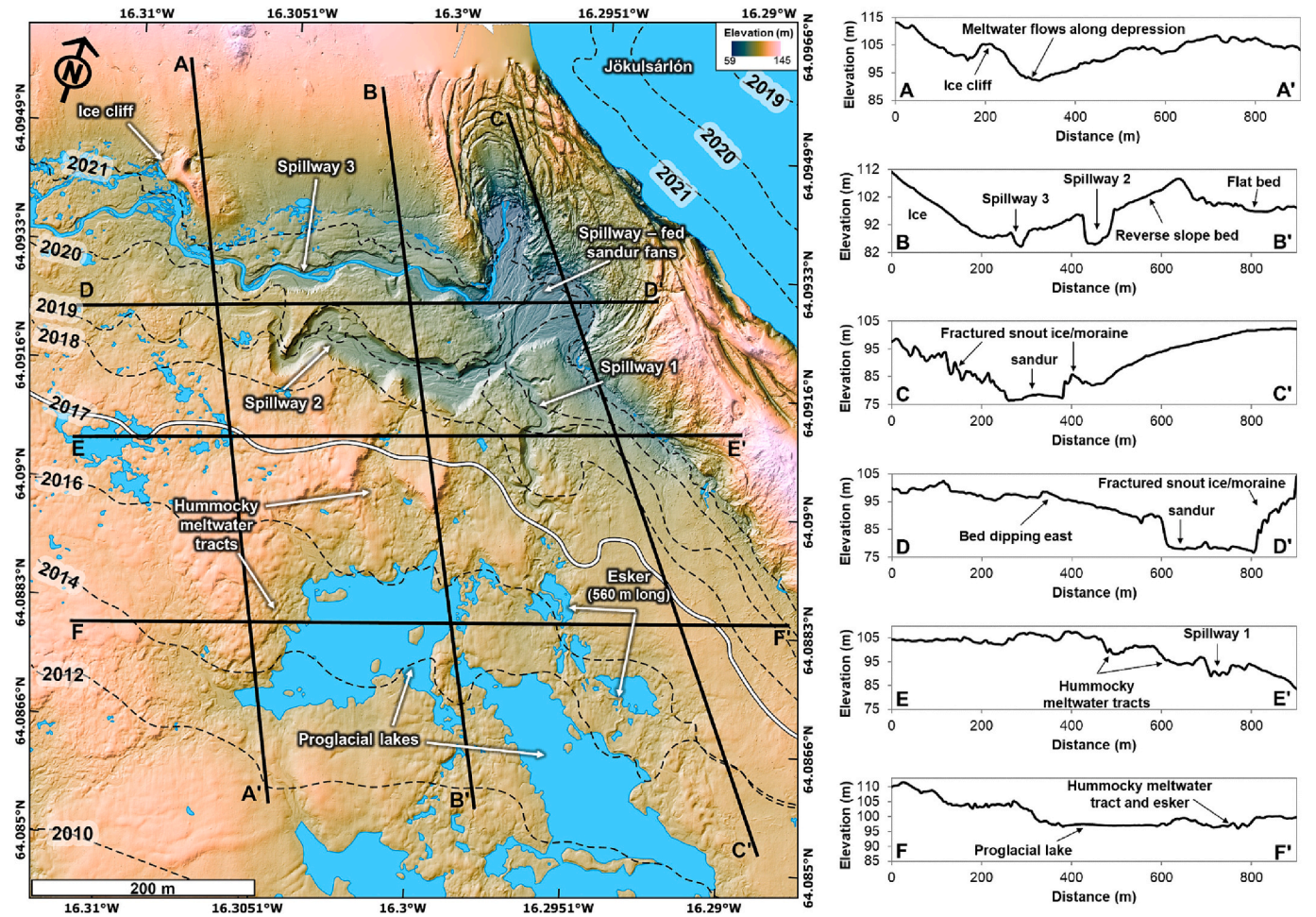

Fig. 6. May 2022 DEM (proglacial water masked in blue) with terminus locations digitised from September Landsat (2010), RapidEye (2012–2018) and Planet (2019–2023) satellite images with profile line locations. Longitudinal profiles A-C highlight that the glacier is retreating into an overdeepening, cross-profiles D and E show the subglacial bed is dipping to the east after 2017, contrasting to the pre-2017 subglacial topography which was dominated by meltwater pooling in depressions across a relatively flat bed. The May 2022 DEM is used as it this dataset covers the entire study area.

The landform assemblage created in response to rapid-ice margin retreat, thinning ice and increased topographic control, no longer includes annual push moraines which were a prominent feature in the Evans and Twigg (2002) active temperate glacier landsystem model.

The glacial geomorphology maps presented in this work (Fig. 5) highlight the rapid geomorphological response to changes in subglacial topography and ice margin stagnation as the glacier snout in the study area has become disconnected from active ice up-glacier following the flow-switch. As deglaciation progresses, the thinning snout and decreasing overburden pressure enables subglacial topography to exert total control on landform development, analogous to neighbouring Fjallsjökull (Chandler et al., 2020b).

5.2. Mechanism for ice marginal spillway initiation

Drainage of ice-contact lakes along the ice margin following the local land-surface gradient initiates the ice margin parallel spillways (Spillways 2–4) (Fig. 9a). A conceptual model, after Utting and Atkinson (2019), is presented in Fig. 8c. Meltwater flowing west to east undercuts the ice margin, resulting in ice collapse and the formation of an ice cliff (Fig. 9d). The emerging topography prevents free drainage to the south, so meltwater pools to form ice-contact lakes. These lakes overflow and drain towards the local topographic low (i.e. towards Jökulsárlón), allowing the hydraulic head to initiate the formation of spillways where meltwater erodes into unconsolidated sediments. These spillways remain active until the ice retreats far enough to create a new ice contact lake at a lower elevation. A new spillway is initiated and the older one is abandoned, and so on. This is consistent with the conceptual model presented by Utting and Atkinson (2019) of proglacial lake formation at the LIS margins in areas retreating across a reverse slope bed. Similar to lateral meltwater channels examined by Syverson and Mickelson (2009) at the downwasting temperate Burroughs Glacier, Alaska, the rate of spillway formation is a function of the slope of the emerging topography, rates of ice retreat/downwasting, substrate erodibility and meltwater supply. The repeat mapping of the Breiðamerkurjökull ice margin allows us to track the development of these spillways and link them with the dominant processes of ice-margin retreat and meltwater impoundment. The results from this contemporary landsystem investigation provides a supporting modern analogue for the model proposed by Utting and Atkinson (2019), improving our confidence of reconstructions of mid-latitude ice sheet dynamics.

5.3. Mechanism for ice flow parallel spillway initiation

Esker deposition in the stable tunnel, Landsystem A, ceased between 2016 and 2017. Spillway 1 is then initiated along the trajectory of the esker, having a longitudinal profile that dips towards the ice margin and marks the point at which the bed begins to dip upglacier.

Satellite images show ice-contact lakes at Spillway 1 were dammed by the ice margin to the north and the Esjufjallajökull moraine to the

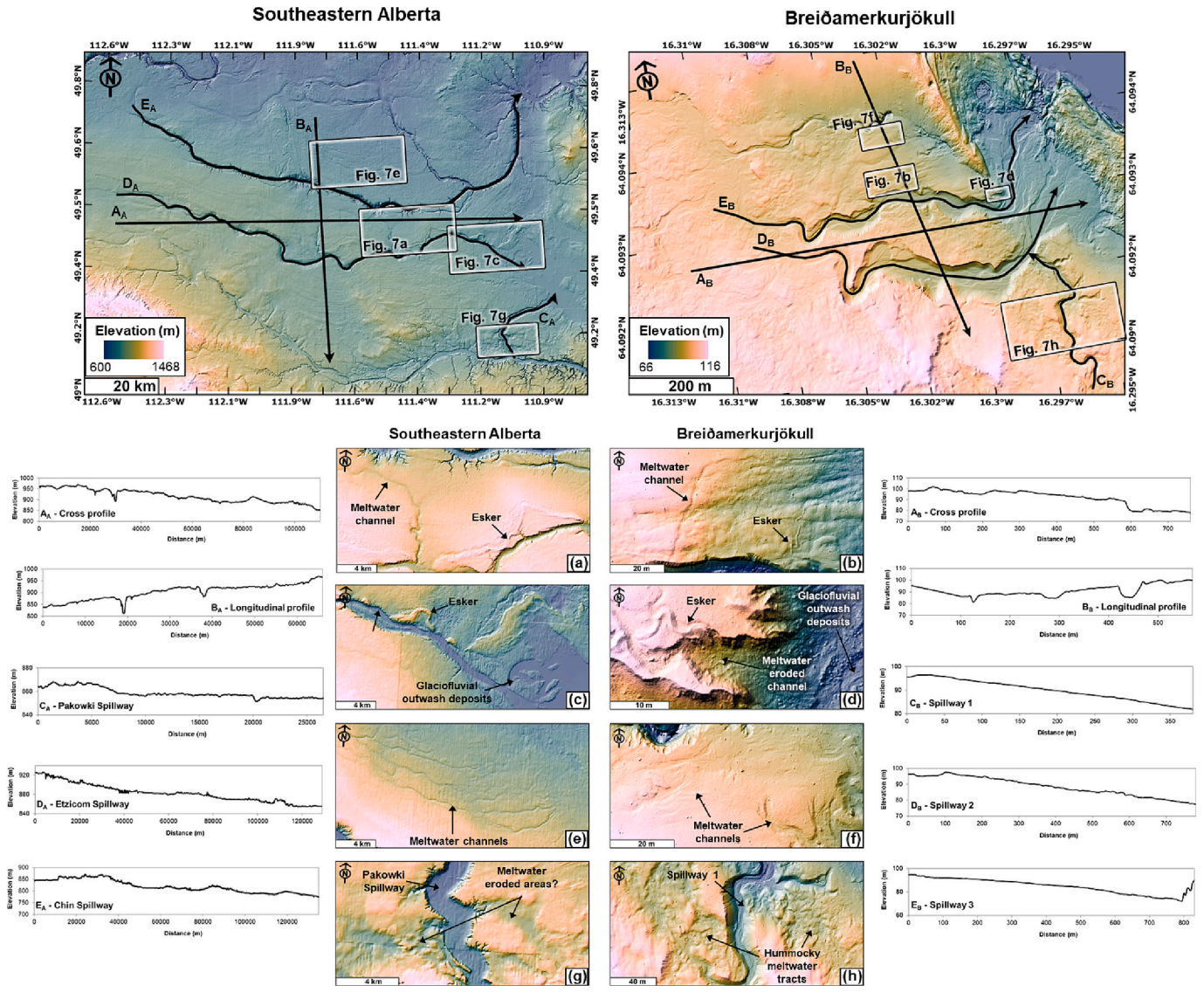

Fig. 7. Profile locations across the Southeastern Alberta and Breiðamerkurjökull study sites. Profile lines include longitudinal profiles of the main spillways. The cross-profile lines A across both study areas indicate that both areas dip to the east, whilst the longitudinal profiles B indicate the foreland also dips northwards with ice-marginal channel incisions. The Pakowki Spillway and Spillway 1 dip towards the depressions. The Etizkom and Chin Spillways dip towards the east and northeast, like Spillways 2 and 3. Comparable geomorphology of Alberta (a, c, e, g) and Breiðamerkurjökull (b, d, f, g,). Relief shaded from highest (pink) to lowest (blue) elevations.

east (Phase 1, Fig. 8b). Similar ice-dammed lakes were common in north-central Alberta as ice retreated down into a palaeo-valley (Slomka and Utting, 2018). We suggest Spillway 1 formed by drainage of these lakes towards the topographic low point in the subglacial bed as the ice retreated (Phase 2, Fig. 8b). Ice contact lakes grow to the point where the water depth exceeds the ice dam overburden stress, then the meltwater exploits the local gradient and begins to drain northwards, down the reverse bed slope under the ice, eroding into the subglacial sediments. This is consistent with the direction of flow across the glaciofluvial outwash fans emanating from the upglacier side of Spillway 1. The drainage of ice contact lakes in 2019 must have occurred through Spillway 1 as they did not flow south, nor did they dry up over such a brief period.

This has implications for assuming channels with profiles dipping towards the ice/palaeo-ice margin are created by pressurised subglacial meltwater flowing uphill along the hydraulic gradient but against the local slope gradient. As the water responsible for erosion of these channels is proglacial or ice-marginal, and not subglacial, subglacial meltwater discharges and subsequent impacts on ice dynamics cannot be inferred from them. Furthermore, these ice-marginal, and at least partially, sub-aerially eroded spillways could serve as analogues for palaeo-ice margins located at the edge of overdeepenings.

5.4. *Breiðamerkurjökull as a modern analogue for the Pakowki Lake Region*

This study presents a high resolution spatio-temporal record documenting ice margin changes at Breiðamerkurjökull and provides a modern analogue for the Pakowki Lake region in Southeast Alberta where meltwater dynamics and landform development was also controlled by subglacial topography (Evans et al., 2014). We acknowledge the significant mismatch of spatiotemporal scales associated with landform development at our ~ 1.5 km^2 Breiðamerkurjökull site and the ~ 35,000 km^2 Alberta study region. We suggest the comparison is justified based on the similarities between the topographic setting (i.e. the presence of a reverse slope bed) and landform assemblage (i.e. ice-marginal spillways created by meltwater impoundment on the ice margin), despite spatiotemporal and climatic (maritime vs continental)

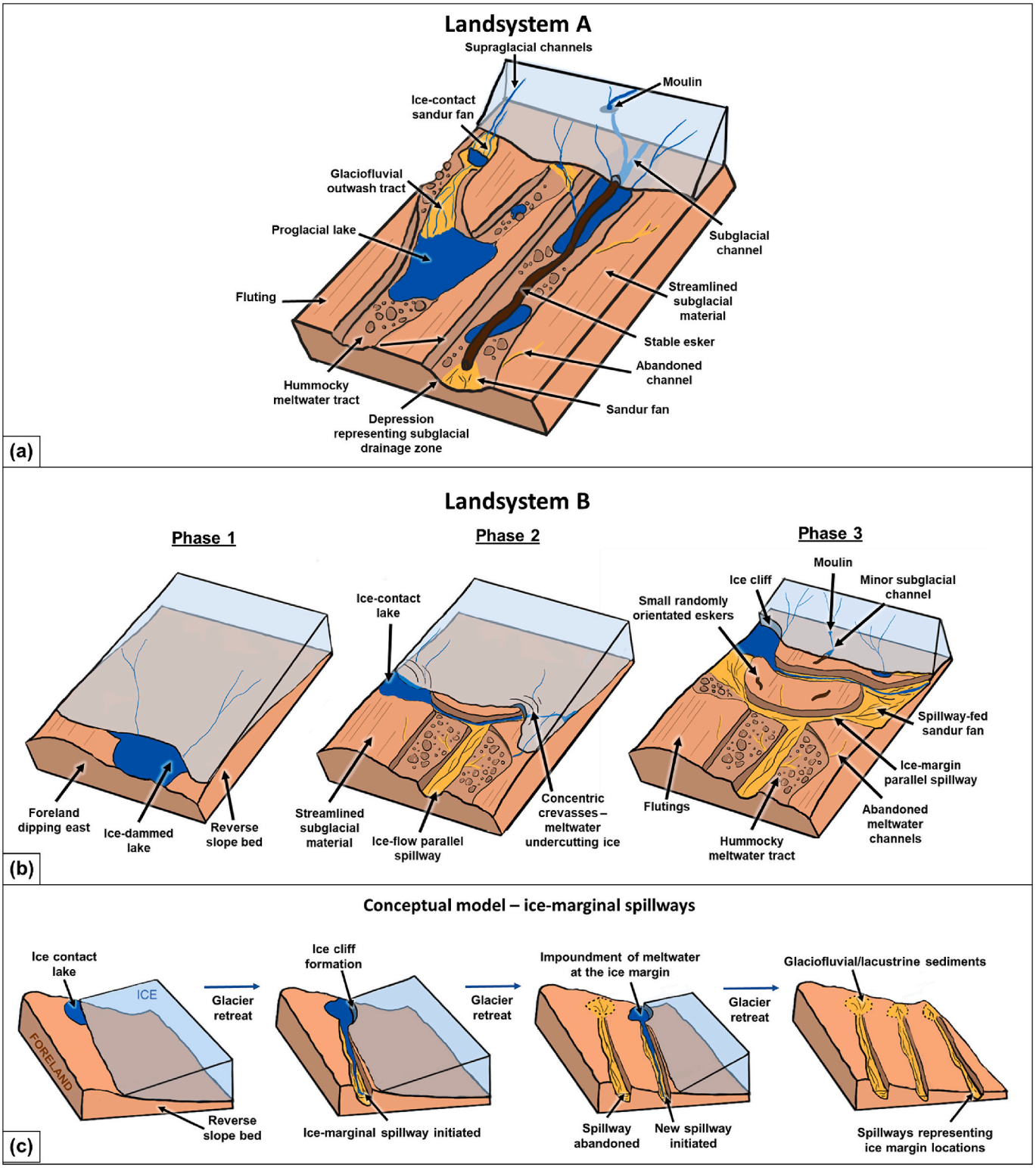

Fig. 8. a) Landsystem A: Landsystem model for the Breiðamerkurjökull study area uncovered from 2010 to 2017 when the glacier was retreating across flat bed topography; b) Landsystem B: Landsystem model for the study area uncovered from 2018 to 2023 as the glacier retreats across a reverse slope bed. Ice dammed lake forms at the edge of an overdeepened area (Phase 1) which drains northwards towards a topographic low point in the bed as the ice retreats (Phase 2) and topographically controlled ice marginal spillways drain water from west to east (Phase 3) and c) conceptual model for meltwater impounding at the ice margin resulting in ice marginal spillways initiated as the glacier retreats across a reverse slope bed, after Utting and Atkinson (2019).

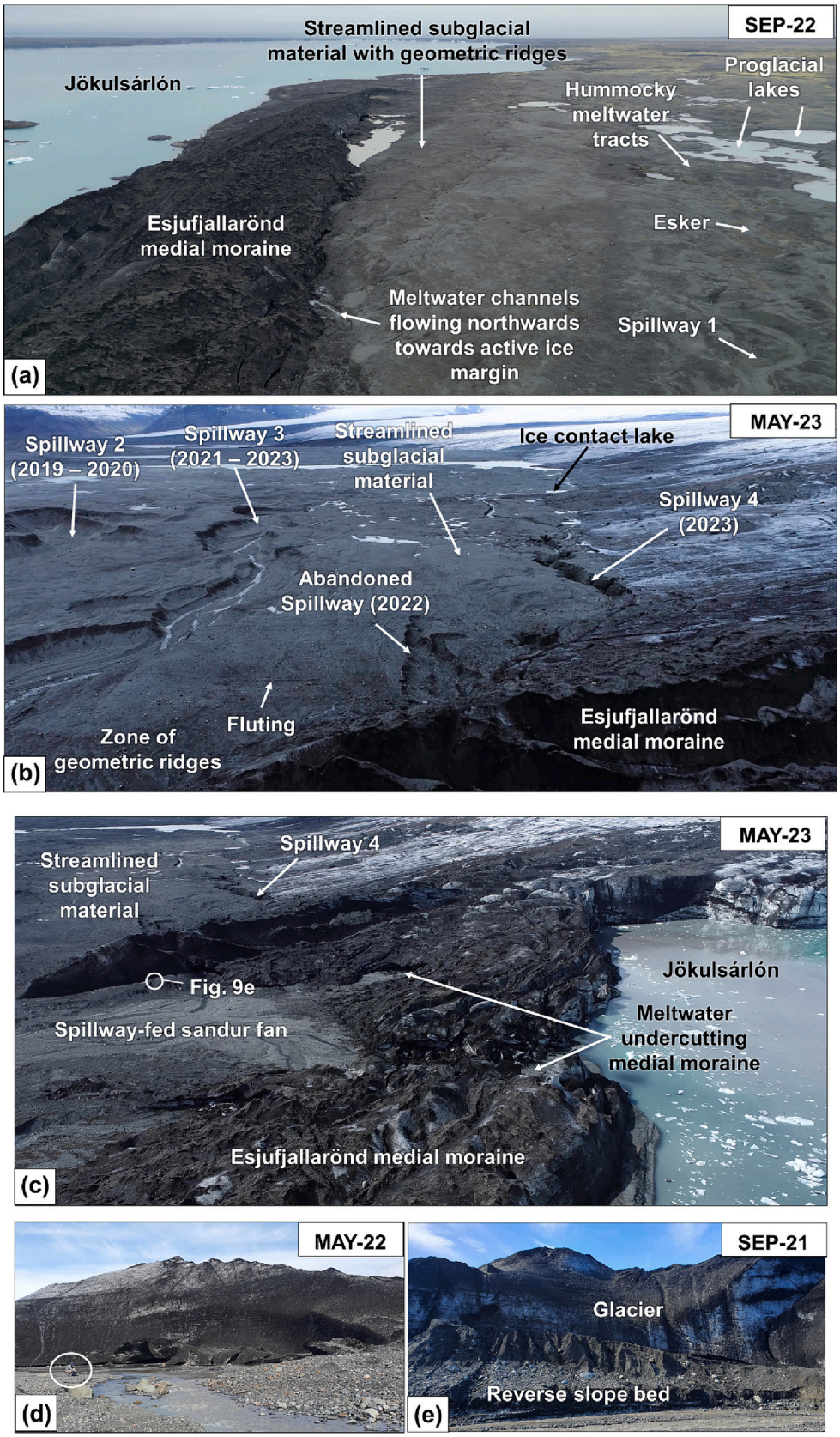

Fig. 9. a) UAV photo of the south foreland area highlighting the landform assemblage across the central flow unit foreland that uncovered mostly before 2017 (photo facing south); b) UAV image of the 2023 ice margin and foreland, with ice margin parallel spillways (photo facing east); c) UAV image of the collapsing ice-cored moraine area undercut by meltwater now flowing into Jökulsárlón (photo facing northeast); d)field photo of the ice cliff developed from meltwater undercutting the margin west of the spillways, person circled for scale (photo facing north); e) field photo of the reverse bed below the glacier (photo facing west).

differences.

Our work supports interpretations by Westgate (1968) and Kulig (1996) for the Pakowki Lake area in Alberta. It contradicts the subglacial origin attributed to the spillways in the region by Beaney (2002). The ice streaming-shutdown dynamic of the Central Alberta Ice Stream (Evans et al., 2014) could have led to a stagnant ice margin consistent with current conditions at Breiðamerkurjökull. The short low relief eskers and preservation of ice-flow direction indicators (i.e. flutings) in the areas between the ice marginal channels provide further evidence to support a stagnant ice margin in the Pakowki Laker region during deglaciation.

In both locations the stagnating ice margin and reverse slope bed forced the formation of ice-contact lakes which subsequently drained towards topographic low points, either below or laterally across the ice margin, eroding deep spillways in the process. With continued retreat across a reverse subglacial bed, the cyclical formation of these spillways in Iceland corroborates the conceptual model of Utting and Atkinson (2019). Furthermore an at least partially subaerial ice-marginal origin for these spillways requires fewer assumptions than a subglacial origin (Evans et al., 2013).

It is proposed that the Etzikom and Chin spillways were formed during deglaciation, whereby meltwater flowed from the west along the edge of the ice margin towards the northeast, following the regional topographic gradient, mostly subaerially, and eroded ice-marginal spillways, as observed at Breiðamerkurjökull (Westgate, 1968; Kulig, 1996). These spillways may also have cut beneath the ice sheet margin becoming submarginal (but not pressurised) at times (Sjogren and Rains, 1995) as drainage pathways are strongly controlled by the northeasterly dip of the bed beneath the retreating ice sheet Evans et al., 2014). This process was observed at Breiðamerkurjökull for Spillway 4 in May 2023 (Phase 2, Fig. 8b). At the modern glacier, spillways are eroded and initiated quasi-annually unlike spillways at the margins of the deglaciating Laurentide Ice Sheet that may have formed over longer timescales. Therefore, it is important to consider the limitations, primarily due to the spatiotemporal mismatch, of scaling up processes at modern glaciers to ice sheet scale.

The interpretation of the ice marginal spillways is consistent with the proglacial lake reconstruction by Utting and Atkinson (2019), whereby Glacial Lake Lethbridge drained through the Etzikom Spillway around 12.3 ka BP (Evans et al., 2014). Glacial Lake Taber drained through the Chin and Forty Mile Spillways (Utting and Atkinson, 2019) (Fig. 2). This sequence of events accounts for the relationship between glaciolacustrine deposits (Evans et al., 2012), channel orientation and the ice margin chronology of the region (Dalton et al., 2020).

Although previous work suggested Glacial Lake Pakowki drained through the Pakowki Spillway (Westgate, 1968; Beaney, 2002), our work suggests that Spillway 1 is an analogue for its formation, whereby meltwater pooled against the ice margin as it retreated off the preglacial watershed. The Pakowki Spillway, which dips back towards the palaeo-ice margin, was initiated as the ice-contact lake drained northeast, beneath the ice margin, towards the Pakowki subglacial depression. Our interpretation for the formation of the Pakowki Spillway aligns with the majority of tunnel valley interpretations along southern margins of LIS by Livingstone and Clark (2016) whereby their formation is driven by gradual upglacier erosion as ice-marginal lakes drain.

Glacial isostatic adjustment (GIA) is important to incorporate into empirical research of palaeo-glaciated terrain to ensure more accurate reconstructions of ice and meltwater dynamics (Godbout et al., 2023). To investigate how isostatic rebound may have influenced the Albertan spillway profiles presented in Fig. 7, we compared the present-day DEM to the 1 km rebound surfaces interpolated from three GIA models by Godbout et al. (2023).

The 25 m Alberta DEM was resampled to 1 km resolution for comparison with the rebound surface representing 14 ka BP. The elevation range across the study site was 741–1526 m 14 ka BP compared to 601–1464 m at present, indicating the region has undergone negative isostatic rebound or isostatic subsidence since deglaciation. The land deformation model (ICE-5G) indicates that this Pakowki Lake area was up to 200 m higher than present when these spillways were initiated during deglaciation ~14–14.5 ka BP. In models ICE-6G and ICE-7G the spillways sit between the 0 and 100 m contours. The deformation raster from the ICE-5G model, indicate vertical displacement of ~ 10 m in the south of the Pakowki Lake region (i.e. extent in Fig. 2b) and up to ~ 140 m to the north, above the Forty Mile Spillway. In the other two models, the deformation ranged from −45 m to 88 m (ICE-6G) and − 55 to 62 m (ICE-7G). While the uplift/subsidence to present could impact the interpretation of ice-flow parallel channel profiles (i.e. the Pakowki spillway), which are parallel to the glacio-isostatic tilt, it is unlikely to affect the ice-marginal spillways (i.e. Chin and Etzikom spillways), which are parallel to the isobase contours. Nonetheless, and although, the 1 km pixel resolution cannot resolve the longitudinal profiles of the channels ~ 14 ka BP, isostatic rebound (positive or negative) should be considered when interpreting the profiles of these ancient spillways from modern elevation datasets.

Future work could identify similar ice-marginal spillways assemblages across palaeo ice-sheet margins to infer ice-marginal and meltwater dynamics. For example, those associated the Huron-Eerie Lobe of the LIS (e.g. Sodeman et al., 2021), the Fennoscandian ice sheet (e.g. Stroeven et al., 2016; Boyes et al., 2021), the Barents Sea and Scandinavian ice sheets (e.g. Larsen et al., 2006), the Late Midlandian Irish ice sheet (e.g. Delaney, 2022) and Greenland Ice Sheet (e.g. Carrivick et al., 2017).

The increased availability of high-quality elevation data from palaeo-glaciated terrain will allow for further investigations supported by improved process-form models developed at modern glacier margins, leading to better palaeo-ice sheet deglacial reconstructions.

6. Conclusion

The central flow unit (Esjufjallajökull) at Breiðamerkurjökull (southeast Iceland) provides valuable insights into the geomorphic responses to ice margin retreat across a reverse bed slope and glacier flow-switching. This investigation utilised UAVs and satellite imagery to document the evolution of the landscape exposed between 2010 and 2023, with detailed mapping of the ice-margin from 2021 to 2023.

Two contrasting landsystems were identified in the study area. Landsystem A is characterised by landforms emerging as the glacier retreats across a flat bed, whereas Landsystem B dominates as the glacier retreats across a reverse slope bed.

Landsystem A contains eskers and hummocky topography in ice flow parallel depressions, representing major subglacial meltwater routes along with areas of streamlined subglacial material. Meltwater flows away from the ice margin under this scenario.

From 2018 central part of the ice margin has become disconnected from the active ice up-glacier and now retreats across a reverse slope bed, which generated a different geomorphological signature. For Landsystem B the emerging topography restricts water flow resulting in the formation of ice-contact lakes, which then drain through ice-marginal spillways eroded into sediments. As the ice retreats, a lake forms at the new margin and initiates a new ice-marginal spillway, and so on. Landsystem B provides a modern analogue for palaeo ice-marginal spillways and are compared to the Pakowki Lake region in Southeast Alberta. Our observations provide evidence to support existing process-form models proposed for the formation of regional sequences of spillways.

This work highlights the role of local topography in driving landform development at downwasting temperate glacier ice margins along with the value of repeatedly surveying landscapes to refine process-form models.

CRediT authorship contribution statement

Amy Lally: Writing – original draft, Visualization, Methodology, Investigation, Funding acquisition, Formal analysis, Conceptualization. **Alastair Ruffell:** Writing – review & editing, Supervision. **Andrew M. W. Newton:** Writing – review & editing, Supervision, Funding acquisition. **Brice R. Rea:** Writing – review & editing, Supervision. **Matteo Spagnolo:** Supervision, Writing – review & editing. **Robert D. Storrar:** Funding acquisition, Methodology, Supervision, Writing – review & editing. **Thorsten Kahlert:** Data curation, Methodology, Resources, Software. **Conor Graham:** Methodology, Resources.

Declaration of competing interest

The authors declare that they have no known competing financial interests or personal relationships that could have appeared to influence the work reported in this paper.

Data availability

Data will be made available on request.

Acknowledgements

AL was funded by UKRI QUADRAT DTP studentship (NE/S007377/1). British Society of Geomorphology Early Career Researcher fund received by AMWN with RDS funding from the Quaternary Research Association. We wish to thank Martin Ross and one anonymous reviewer for their valuable input and suggestions, which improved the quality of the manuscript. We are especially grateful to Sigurður Jónsson of Vatnajökull National Park for supplying our research permits and site advice.

References

Ahokangas, E., Ojala, A.E.K., Tuunainen, A., Valkama, M., Palmu, J.P., Kajuutti, K., Mäkinen, J., 2021. The distribution of glacial meltwater routes and associated murtoo fields in Finland. Geomorphology 389. https://doi.org/10.1016/j.geomorph.2021.107854.

Alley, R.B., Anandakrishnan, S., Bentley, C.R., Lord, N., 1994. A water-piracy hypothesis for the stagnation of Ice Stream C, Antarctica. Ann. Glaciol. 20, 187–194. https://doi.org/10.3189/1994aog20-1-187-194.

Anandakrishnan, S., Alley, R.B., 1997. Stagnation of ice stream C, West Antarctica by water piracy. Geophys. Res. Lett. 24, 265–268. https://doi.org/10.1029/96GL04016.

Atkinson, N., Utting, D.J., Pawley, S.M., 2014. Glacial Landforms of Alberta.

Atkinson, N., Utting, D.J., Pawley, S.M., 2018. Glacial landforms of Alberta, Canada, version 3.0 (GIS data, line features); Alberta Energy Regulator, AER/AGS Digital Dataset 2014-0022.

Aylsworth, J.M., Shilts, W.W., 1989. Bedforms of the Keewatin Ice Sheet, Canada. Sediment. Geol. 62, 407–428. https://doi.org/10.1016/0037-0738(89)90129-2.

Bamber, J.L., Vaughan, D.G., Joughin, I., 2000. Widespread complex flow in the interior of the antarctic ice sheet. Science 1979 (287), 1248–1250. https://doi.org/10.1126/science.287.5456.1248.

Baurley, N.R., Robson, B.A., Hart, J.K., 2020. Long-term impact of the proglacial lake Jökulsárlón on the flow velocity and stability of Breiðamerkurjökull glacier, Iceland. Earth Surf. Process. Landf. 45, 2647–2663. https://doi.org/10.1002/esp.4920.

Beaney, C.L., 2002. Tunnel channels in Southeast Alberta, Canada: evidence for catastrophic channelized drainage. Quat. Int. 90, 67–74. https://doi.org/10.1016/S1040-6182(01)00093-3.

Beaney, C.L., Shaw, J., 2000. The subglacial geomorphology of Southeast Alberta: evidence for subglacial meltwater erosion. Can. J. Earth Sci. 37, 51–61. https://doi.org/10.1139/e99-112.

Bennett, G.L., Evans, D.J.A., 2012. Glacier retreat and landform production on an overdeepened glacier foreland: the debris-charged glacial landsystem at Kvíárjökull, Iceland. Earth Surf. Process. Landf. 37, 1584–1602. https://doi.org/10.1002/ESP.3259.

Björnsson, H., 1996. 300 m deep trench created beneath Breiðamerkurjökull during the Little Ice Age. Ann. Glaciol. 111, 141–146.

Björnsson, H., Pálsson, F., 2008. Icelandic glaciers. Jökull 58, 365–386.

Björnsson, H., Pálsson, F., 2020. Radio-echo soundings on Icelandic temperate glaciers: history of techniques and findings. Ann. Glaciol. 61, 25–34. https://doi.org/10.1017/aog.2020.10.

Boulton, G.S., Lunn, R., Vidstrand, P., Zatsepin, S., 2007a. Subglacial drainage by groundwater-channel coupling, and the origin of esker systems: part 1-glaciological observations. Quat. Sci. Rev. 26, 1067–1090. https://doi.org/10.1016/j.quascirev.2007.01.007.

Boulton, G.S., Lunn, R., Vidstrand, P., Zatsepin, S., 2007b. Subglacial drainage by groundwater-channel coupling, and the origin of esker systems: part II-theory and simulation of a modern system. Quat. Sci. Rev. 26, 1091–1105. https://doi.org/10.1016/j.quascirev.2007.01.006.

Boyes, B.M., Pearce, D.M., Linch, L.D., 2021. Glacial geomorphology of the Kola Peninsula and Russian Lapland. J. Maps 17, 485–503. https://doi.org/10.1080/17445647.2021.1970036.

Brandon, M., Hodgkins, R., Björnsson, H., Olafsson, J., 2017. Multiple melt plumes observed at the Breiðamerkurjökull ice face in the upper waters of Jökulsárlón lagoon, Iceland. Ann. Glaciol. 58, 131–143. https://doi.org/10.1017/aog.2017.10.

Brennand, T.A., Shaw, J., 2011. Tunnel channels and associated landforms, south-central Ontario: their implications for ice-sheet hydrology, 10.1139/e94-045 31, 505–522. 10.1139/E94-045.

Briner, J.P., Bini, A.C., Anderson, R.S., 2009. Rapid early Holocene retreat of a Laurentide outlet glacier through an Arctic fjord. Nat. Geosci. 2, 496–499. https://doi.org/10.1038/ngeo556.

Briner, J.P., Cuzzone, J.K., Badgeley, J.S., Young, N.E., Steig, E.J., Morlighem, M., Schlegel, N.-J., Hakim, G.J., Schaefer, J., Johnson, J.V., Lesnek, A.J., Thomas, E.K., Allan, E., Bennike, O., Cluett, A.A., Csatho, B., de Vernal, A., Downs, J., Larour, E., Nowicki, S., 2020. Greenland Ice Sheet mass loss rate will exceed Holocene values this century. Nature 586, 40–74. https://doi.org/10.1038/s41586-020-2742-6.

Brouard, E., Lajeunesse, P., 2019. Ice-stream flow switching by up-ice propagation of instabilities along glacial marginal troughs. Cryosphere 13, 981–996. https://doi.org/10.5194/tc-13-981-2019.

Carrivick, J.L., Yde, J., Russell, A.J., Quincey, D.J., Ingeman-Nielsen, T., Mallalieu, J., 2017. Ice-margin and meltwater dynamics during the mid-Holocene in the Kangerlussuaq area of West Greenland. Boreas 46, 369–387. https://doi.org/10.1111/bor.12199.

Chandler, B.M.P., Lovell, H., Boston, C.M., Lukas, S., Barr, I.D., Benediktsson, Í.Ö., Benn, D.I., Clark, C.D., Darvill, C.M., Evans, D.J.A., Ewertowski, M.W., Loibl, D., Margold, M., Otto, J.C., Roberts, D.H., Stokes, C.R., Storrar, R.D., Stroeven, A.P., 2018. Glacial geomorphological mapping: a review of approaches and frameworks for best practice. Earth Sci. Rev. 185, 806–846. https://doi.org/10.1016/j.earscirev.2018.07.015.

Chandler, B.M.P., Chandler, S.J.P., Evans, D.J.A., Ewertowski, M.W., Lovell, H., Roberts, D.H., Schaefer, M., Tomczyk, A.M., 2020a. Sub-annual moraine formation at an active temperate Icelandic glacier. Earth Surf. Process. Landf. 45, 1622–1643. https://doi.org/10.1002/esp.4835.

Chandler, B.M.P., Evans, D.J.A., Chandler, S.J.P., Ewertowski, M.W., Lovell, H., Roberts, D.H., Schaefer, M., Tomczyk, A.M., 2020b. The glacial landsystem of Fjallsjökull, Iceland: Spatial and temporal evolution of process-form regimes at an active temperate glacier. Geomorphology 361, 107192. https://doi.org/10.1016/j.geomorph.2020.107192.

Christiansen, E.A., 1977. Glacial Spillways in the Prairies: A Natural History Theme Study of Glacial Spillways in Natural Regions 12, 13 and 14. Saskatoon.

Clark, P.U., Walder, J.S., 1994. Subglacial drainage, eskers, and deforming beds beneath the Laurentide and Eurasian ice sheets. Geol. Soc. Am. Bull. 106, 304–314. https://doi.org/10.1130/0016-7606(1994)106<0304:SDEADB>2.3.CO;2.

Conway, H., Catania, G., Raymond, C.F., Gades, A.M., Scambos, T.A., Engelhardt, H., 2002. Switch of flow direction in an antarctic ice stream. Nature 419, 465–467. https://doi.org/10.1038/nature01081.

Couette, P.O., Lajeunesse, P., Ghienne, J.F., Dorschel, B., Gebhardt, C., Hebbeln, D., Brouard, E., 2023. Retreat and stabilization of a marine-based ice margin along a high arctic fjord-cross-shelf trough system. Quat. Sci. Rev. 302, 107949 https://doi.org/10.1016/j.quascirev.2022.107949.

Crameri, F., 2020. Scientific Colour Maps [WWW Document]. URL https://www.fabiocrameri.ch/colourmaps/ (accessed 8.8.22).

Dalton, A.S., Margold, M., Stokes, C.R., Tarasov, L., Dyke, A.S., Adams, R.S., Allard, S., Arends, H.E., Atkinson, N., Attig, J.W., Barnett, P.J., Barnett, R.L., Batterson, M., Bernatchez, P., Borns, H.W., Breckenridge, A., Briner, J.P., Brouard, E., Campbell, J. E., Carlson, A.E., Clague, J.J., Curry, B.B., Daigneault, R.A., Dubé-Loubert, H., Easterbrook, D.J., Franzi, D.A., Friedrich, H.G., Funder, S., Gauthier, M.S., Gowan, A.S., Harris, K.L., Hétu, B., Hooyer, T.S., Jennings, C.E., Johnson, M.D., Kehew, A.E., Kelley, S.E., Kerr, D., King, E.L., Kjeldsen, K.K., Knaeble, A.R., Lajeunesse, P., Lakeman, T.R., Lamothe, M., Larson, P., Lavoie, M., Loope, H.M., Lowell, T.V., Lusardi, B.A., Manz, L., McMartin, I., Nixon, F.C., Occhietti, S., Parkhill, M.A., Piper, D.J.W., Pronk, A.G., Richard, P.J.H., Ridge, J.C., Ross, M., Roy, M., Seaman, A., Shaw, J., Stea, R.R., Teller, J.T., Thompson, W.B., Thorleifson, L.H., Utting, D.J., Veillette, J.J., Ward, B.C., Weddle, T.K., Wright, H.E., 2020. An updated radiocarbon-based ice margin chronology for the last deglaciation of the North American Ice Sheet Complex. Quat Sci Rev 234. https://doi.org/10.1016/j.quascirev.2020.106223.

Delaney, C., 2022. The development and impact of an ice-contact proglacial lake during the Last Glacial Termination, Palaeolake Riada, Central Ireland. J. Quat. Sci. 37, 1422–1441. https://doi.org/10.1002/jqs.3412.

Delaney, C.A., McCarron, S., Davis, S., 2018. Irish Ice Sheet dynamics during deglaciation of the central Irish Midlands: evidence of ice streaming and surging from airborne LiDAR. Geomorphology 306, 235–253. https://doi.org/10.1016/J.GEOMORPH.2018.01.011.

Dewald, N., Lewington, E., Livingstone, S.J., Clark, C.D., Storrar, R.D., 2021. Distribution, Characteristics and Formation of Esker Enlargements. Geomorphology. https://doi.org/10.1016/j.geomorph.2021.107919.

Dewald, N., Livingstone, S.J., Clark, C.D., 2022. Subglacial meltwater routes of the Fennoscandian Ice Sheet. https://doi.org/10.1080/17445647.2022.2071648.

Dowdeswell, J.A., Ottesen, D., Rise, L., 2006. Flow switching and large-scale deposition by ice streams draining former ice sheets. Geology 34, 313–316. https://doi.org/10.1130/G22253.1.
Ely, J.C., Clark, C.D., Ng, F.S.L., Spagnolo, M., 2017. Insights on the formation of longitudinal surface structures on ice sheets from analysis of their spacing, spatial distribution, and relationship to ice thickness and flow. Case Rep. Med. 122, 961–972. https://doi.org/10.1002/2016JF004071.
Etzelmüller, B., Farbrot, H., Guomundsson, Á., Humlum, O., Tveito, O.E., Björnsson, H., 2007. The regional distribution of mountain permafrost in Iceland. Permafr. Periglac. Process. 18, 185–199. https://doi.org/10.1002/ppp.583.
Evans, D.J.A., 2000. Quaternary geology and geomorphology of the Dinosaur Provincial Park area and surrounding plains, Alberta, Canada: the identification of former glacial lobes, drainage diversions and meltwater flood tracks. Quat. Sci. Rev. 19, 931–958. https://doi.org/10.1016/S0277-3791(99)00029-3.
Evans, D.J.A., 2011. Glacial Landsystems of Satujökull, Iceland: A modern analogue for glacial landsystem overprinting by mountain icecaps. Geomorphology. https://doi.org/10.1016/j.geomorph.2011.01.025.
Evans, D.J.A., Twigg, D.R., 2000. Breiðamerkurjökull 1998. 1:30,000 Scale Map. University of Glasgow and Loughborough University.
Evans, D.J.A., Twigg, D.R., 2002. The active temperate glacial landsystem: a model based on Breiðamerkurjökull and Fjallsjökull, Iceland. Quat. Sci. Rev. 21, 2143–2177. https://doi.org/10.1016/S0277-3791(02)00019-7.
Evans, D.J.A., Lemmen, D.S., Rea, B.R., 1999. Glacial landsystems of the southwest Laurentide ice sheet: Modern Icelandic analogues. J. Quat. Sci. 14, 673–691. https://doi.org/10.1002/(sici)1099-1417(199912)14:7<673::aid-jqs467>3.0.co;2-%23.
Evans, D.J.A., Clark, C., Rea, B., 2008. Landform and sediment imprints of fast glacier flow in the southwest Laurentide Ice Sheet. https://doi.org/10.1002/JQS.1141.
Evans, D.J.A., Hiemstra, J.F., Boston, C.M., Leighton, I., Cofaigh, C.Ó., Rea, B.R., 2012. Till stratigraphy and sedimentology at the margins of terrestrially terminating ice streams: Case study of the western Canadian prairies and high plains. Quat. Sci. Rev. 46, 80–125. https://doi.org/10.1016/j.quascirev.2012.04.028.
Evans, D.J.A., Hiemstra, J.F., Boston, C.M., Leighton, I., Cofaigh, C.Ó., Rea, B.R., 2013. Reply to John Shaw " Correspondence - Alberta flow paths: A need for balance.". Quat. Sci. Rev. 63, 144–148. https://doi.org/10.1016/j.quascirev.2012.12.011.
Evans, D.J.A., Young, N.J.P., Cofaigh, C.O., 2014. Glacial geomorphology of terrestrial-terminating fast flow lobes/ice stream margins in the southwest Laurentide Ice Sheet. Geomorphology 204, 86–113. https://doi.org/10.1016/j.geomorph.2013.07.031.
Evans, D., Storrar, R., Rea, B., 2016a. Crevasse-squeeze ridge corridors: Diagnostic features of late-stage palaeo-ice stream activity. Geomorphology 258. https://doi.org/10.1016/j.geomorph.2016.01.017.
Evans, D.J.A., Ewertowski, M., Orton, C., 2016b. Fláajökull (north lobe), Iceland: active temperate piedmont lobe glacial landsystem. J. Maps 12, 777–789. https://doi.org/10.1080/17445647.2015.1073185.
Evans, D.J.A., Atkinson, N., Phillips, E., 2020. Glacial geomorphology of the Neutral Hills Uplands, Southeast Alberta, Canada: the process-form imprints of dynamic ice streams and surging ice lobes. Geomorphology 350. https://doi.org/10.1016/j.geomorph.2019.106910.
Evans, D.J.A., Ewertowski, M.W., Tomczyk, A., Chandler, B.M.P., 2023. Active temperate glacial landsystem evolution in association with outwash head/depositional overdeepenings. Earth Surf. Process. Landf. https://doi.org/10.1002/ESP.5569.
Eyles, N., 1983. Modern Icelandic glaciers as depositional models for 'hummocky moraine' in the Scottish Highlands. In: Evenson, E.B., Schluchter, C., Rabassa, J. (Eds.), Tills and Related Deposits: Genesis, Petrology, Stratigraphy. Balkema, Rotterdam, pp. 47–60.
Gauthier, M.S., Hodder, T.J., Ross, M., Kelley, S.E., Rochester, A., McCausland, P., 2019. The subglacial mosaic of the Laurentide Ice Sheet; a study of the interior region of southwestern Hudson Bay. Quat. Sci. Rev. 214, 1–27. https://doi.org/10.1016/j.quascirev.2019.04.015.
Gauthier, M.S., Breckenridge, A., Hodder, T.J., 2022. Patterns of ice recession and ice stream activity for the MIS 2 Laurentide Ice Sheet in Manitoba, Canada. Boreas 51, 274–298. https://doi.org/10.1111/BOR.12571.
Godbout, P.M., Brouard, E., Roy, M., 2023. 1-km resolution rebound surfaces and paleotopography of glaciated North America since the Last Glacial Maximum. Sci Data 10. https://doi.org/10.1038/s41597-023-02566-5.
Greenwood, S.L., Clark, C.D., 2009. Reconstructing the last Irish Ice Sheet 2: a geomorphologically-driven model of ice sheet growth, retreat and dynamics. Quat. Sci. Rev. 28, 3101–3123. https://doi.org/10.1016/j.quascirev.2009.09.014.
Greenwood, S.L., Clark, C.D., Hughes, A.L.C., 2007. Formalising an inversion methodology for reconstructing ice-sheet retreat patterns from meltwater channels: Application to the British Ice Sheet. J. Quat. Sci. 22, 637–645. https://doi.org/10.1002/jqs.1083.
Guðmundsson, S., Björnsson, H., 2016. Changes in the flow of Breiðamerkurjökull reflected by bending of the Esjufjallarönd medial moraine. Jökull 66, 95–100.
Guðmundsson, S., Evans, D.J.A., 2022. Geomorphological map of Breiðamerkursandur 2018: the historical evolution of an active temperate glacier foreland. Geogr. Ann. Ser. B. https://doi.org/10.1080/04353676.2022.2148083.
Guðmundsson, S., Björnsson, H., Pálsson, F., Magnússon, E., Sæmundsson, Þ., Jóhannesson, T., 2019. Terminus lakes on the south side of Vatnajökull ice cap, SE-Iceland. Jökull 69, 1–34. https://doi.org/10.33799/jokull2019.69.001.
Guðmundsson, S., Björnsson, H., Pálsson, F., 2017. Changes of Breiðamerkurjökull glacier, SE-iceland, from its late nineteenth century maximum to the present. Geogr. Ann. Ser. B 99, 338–352. https://doi.org/10.1080/04353676.2017.1355216.
Howarth, P.J., Welch, R., 1969a. Breiðamerkurjökull, South-east Iceland, August 1945. 1:30,000 scale map. University of Glasgow.
Howarth, P.J., Welch, R., 1969b. Breiðamerkurjökull, South-east Iceland, August 1965. 1:30,000 scale map. University of Glasgow.
Hulbe, C., Fahnestock, M., 2007. Century-scale discharge stagnation and reactivation of the Ross ice streams, West Antarctica. Case Rep. Med. 112, 1–11. https://doi.org/10.1029/2006JF000603.
Jansson, K.N., 2003. Early Holocene glacial lakes and ice marginal retreat pattern in Labrador/Ungava, Canada. Palaeogeogr. Palaeoclimatol. Palaeoecol. 193, 473–501. https://doi.org/10.1016/S0031-0182(03)00262-1.
Kleman, J., Borgström, I., 1996. Reconstruction of palaeo-ice sheets: the use of geomorphological data. Earth Surf. Process. Landf. 21, 893–909. https://doi.org/10.1002/(SICI)1096-9837(199610)21:10<893::AID-ESP620>3.0.CO;2-U.
Kulig, J.J., 1996. The glaciation of the Cypress Hills of Alberta and Saskatchewan and its regional implications. Quat. Int. 32, 53–77. https://doi.org/10.1016/1040-6182(95)00059-3.
Lally, A., Ruffell, A., Newton, A.M.W., Rea, B.R., Kahlert, T., Storrar, R.D., Spagnolo, M., Graham, C., Coleman, M., 2023. The evolution and preservation potential of englacial eskers: an example from Breiðamerkurjökull. SE Iceland. Earth Surf Process Landf 1–20. https://doi.org/10.1002/esp.5664.
Larsen, E., Kjær, K., Demidov, I., Funder, S., Grøsfjeld, K., Houmark-Nielsen, M., Jensen, M., Linge, H., Lysså, A., 2006. Late pleistocene glacial and lake history of northwestern Russia. Boreas 35 (3), 394–424. https://doi.org/10.1080/03009480600781958.
Livingstone, S.J., Clark, C.D., 2016. Morphological properties of tunnel valleys of the southern sector of the Laurentide Ice Sheet and implications for their formation. Earth Surf. Dyn. 4, 567–589. https://doi.org/10.5194/esurf-4-567-2016.
Newton, A.M.W., Huuse, M., 2017. Glacial geomorphology of the central Barents Sea: Implications for the dynamic deglaciation of the Barents Sea Ice Sheet. https://doi.org/10.1016/j.margeo.2017.04.001.
Ó Cofaigh, C., Evans, D.J.A., Smith, I.R., 2010. Large-scale reorganization and sedimentation of terrestrial ice streams during late Wisconsinan Laurentide Ice Sheet deglaciation. Geol. Soc. Am. Bull. 122, 743–756.
Ojala, A.E.K., Mäkinen, J., Ahokangas, E., Kajuutti, K., Valkama, M., Tuunainen, A., Palmu, J.P., 2021. Diversity of murtoos and murtoo-related subglacial landforms in the Finnish area of the Fennoscandian Ice Sheet. Boreas 50, 1095–1115. https://doi.org/10.1111/bor.12526.
Payne, A.J., Dongelmans, P.W., 1997. Self-organization in the thermomechanical flow of ice sheets. J. Geophys. Res. Solid Earth 102, 12219–12233. https://doi.org/10.1029/97JB00513.
Price, R.J., 1969. Moraines, Sandar, Kames and Eskers near Breiðamerkurjökull, Iceland. Trans. Inst. Br. Geogr. 46, 17–43.
Price, R.J., 1971. The development and destruction of a Sandur, Breiðamerkurjökull, Iceland. Arct. Alp. Res. 3, 225–237.
Price, R.J., 1982. Changes in the proglacial area of Breiðamerkurjökull, southeastern Iceland: 1890–1980. Jökull 32, 29–35.
Price, R.J., Howarth, P.J., 1970. The evolution of the drainage system (1904–1965) in front of Breiðamerkurjökull, Iceland. Jökull 20, 27–37.
Rea, B.R., Evans, D.J.A., 2011. An assessment of surge-induced crevassing and the formation of crevasse squeeze ridges. Case Rep. Med. 116 https://doi.org/10.1029/2011JF001970.
Regnéll, C., Peterson Becher, G., Öhrling, C., Greenwood, S.L., Gyllencreutz, R., Blomdin, R., Brendryen, J., Goodfellow, B.W., Mikko, H., Ransed, G., Smith, C., 2023. Ice-dammed lakes and deglaciation history of the Scandinavian Ice Sheet in central Jämtland, Sweden. Quat. Sci. Rev. 314 https://doi.org/10.1016/j.quascirev.2023.108219.
Rice, J.M., Paulen, R.C., Campbell, H.E., Ross, M., 2024. The surficial geology record of ice stream catchment dynamics and ice-divide migration in the Quebec-Labrador sector of the Laurentide ice sheet. Quaternary Science Advances 13. https://doi.org/10.1016/j.qsa.2023.100123.
Ross, M., Campbell, J.E., Parent, M., Adams Boreas Ross, R.S., Adams, R.S., 2009. Palaeo-ice streams and the subglacial landscape mosaic of the North American mid-continental prairies. Boreas 38, 421–439. https://doi.org/10.1111/j.1502.
Shetsen, I., 1987. Quaternary Geology, Southern Alberta. Alberta Research Council Map, Scale 1:500,000.
Sjogren, D.B., Rains, R.B., 1995. Glaciofluvial erosional morphology and sediments of the Coronation-Spondin scabland, east-central Alberta. Can. J. Earth Sci. 32, 565–578.
Śledź, S., Ewertowski, M., Piekarczyk, J., 2021. Applications of unmanned aerial vehicle (UAV) surveys and Structure from Motion photogrammetry in glacial and periglacial geomorphology. Geomorphology 378, 107620. https://doi.org/10.1016/j.geomorph.2021.107620.
Śledź, S., Ewertowski, M.W., Evans, D.J.A., 2023. Quantification of Short-Term Transformations of Proglacial Landforms in a Temperate, Debris-Charged Glacial Landsystem, Kvíárjökull, Iceland. Land Degrad Dev. https://doi.org/10.1002/ldr.4865.
Slomka, J.M., Utting, D.J., 2018. Glacial advance, occupation and retreat sediments associated with multi-stage ice-dammed lakes: north-Central Alberta, Canada. Boreas 47, 150–174. https://doi.org/10.1111/bor.12257.
Sodeman, A.D., Fisher, T.G., Wolfe, E.R., Becker, R.H., Martin-Hayden, J.M., Loope, H. M., 2021. Parallel tunnel channels of the Huron-Erie Lobe of the Laurentide Ice Sheet: a variation of tunnel channels with implications on lobe history and subglacial meltwater dynamics. Geomorphology 385, 107726. https://doi.org/10.1016/j.geomorph.2021.107726.
Stokes, C.R., Clark, C.D., 2004. Evolution of late glacial ice-marginal lakes on the northwestern Canadian Shield and their influence on the location of the Dubawnt Lake palaeo-ice stream. Palaeogeogr Palaeoclimatol Palaeoecol 215, 155–171. https://doi.org/10.1016/j.palaeo.2004.09.006.

Stokes, C.R., Clark, C.D., Storrar, R., 2009. Major changes in ice stream dynamics during deglaciation of the north-western margin of the Laurentide Ice Sheet. Quat Sci Rev 28, 721–738. https://doi.org/10.1016/j.quascirev.2008.07.019.

Stokes, C.R., Tarasov, L., Dyke, A.S., 2012. Dynamics of the North American Ice Sheet Complex during its inception and build-up to the Last Glacial Maximum. Quat. Sci. Rev. 50, 86–104. https://doi.org/10.1016/j.quascirev.2012.07.009.

Stokes, C.R., Corner, G.D., Winsborrow, M.C.M., Husum, K., Andreassen, K., 2014. Asynchronous response of marine-terminating outlet glaciers during deglaciation of the Fennoscandian ice sheet. Geology 42, 455–458. https://doi.org/10.1130/G35299.1.

Storrar, R.D., Stokes, C.R., Evans, D.J.A., 2014. Morphometry and pattern of a large sample (>20,000) of Canadian eskers and implications for subglacial drainage beneath ice sheets. Quat Sci Rev 105, 1–25. https://doi.org/10.1016/J.QUASCIREV.2014.09.013.

Storrar, R.D., Evans, D.J.A., Stokes, C.R., Ewertowski, M., 2015. Controls on the location, morphology and evolution of complex esker systems at decadal timescales, Breiðamerkurjökull, Southeast Iceland. Earth Surf. Process. Landf. 40, 1421–1438. https://doi.org/10.1002/esp.3725.

Storrar, R.D., Jones, A.H., Evans, D.J.A., 2017. Small-scale topographically-controlled glacier flow switching in an expanding proglacial lake at Breiðamerkurjökull, SE Iceland. J. Glaciol. 63, 745–750. https://doi.org/10.1017/jog.2017.22.

Stroeven, A.P., Hättestrand, C., Kleman, J., Heyman, J., Fabel, D., Fredin, O., Goodfellow, B.W., Harbor, J.M., Jansen, J.D., Olsen, L., Caffee, M.W., Fink, D., Lundqvist, J., Rosqvist, G.C., Strömberg, B., Jansson, K.N., 2016. Deglaciation of Fennoscandia. Quat Sci Rev 147, 91–121.

Syverson, K.M., Mickelson, D.M., 2009. Origin and significance of lateral meltwater channels formed along a temperate glacier margin, Glacier Bay, Alaska. Boreas 38, 132–145. https://doi.org/10.1111/j.1502-3885.2008.00042.x.

Utting, D.J., Atkinson, N., 2019. Proglacial lakes and the retreat pattern of the southwest Laurentide Ice Sheet across Alberta. Canada. Quat Sci Rev 225, 106034. https://doi.org/10.1016/j.quascirev.2019.106034.

Voytenko, D., Dixon, T.H., Luther, M.E., Lembke, C., Howat, I.M., de la Peña, S., 2015. Observations of inertial currents in a lagoon in southeastern Iceland using terrestrial radar interferometry and automated iceberg tracking. Comput. Geosci. 82, 23–30. https://doi.org/10.1016/j.cageo.2015.05.012.

Westgate, J.A., 1968. Surficial Geology of the Foremost-Cypress Hills Area, Alberta. Alberta Research Council, Bulletin.

Westoby, M.J., Brasington, J., Glasser, N.F., Hambrey, M.J., Reynolds, J.M., 2012. "Structure-from-Motion" photogrammetry: a low-cost, effective tool for geoscience applications. Geomorphology 179, 300–314. https://doi.org/10.1016/j.geomorph.2012.08.021.

Winsborrow, M.C.M., Stokes, C.R., Andreassen, K., 2012. Ice-stream flow switching during deglaciation of the southwestern Barents Sea. Bull. Geol. Soc. Am. 124, 275–290. https://doi.org/10.1130/B30416.1.

Young, N.E., Briner, J.P., Miller, G.H., Lesnek, A.J., Crump, S.E., Thomas, E.K., Pendleton, S.L., Cuzzone, J., Lamp, J., Zimmerman, S., Caffee, M., Schaefer, J.M., 2020. Deglaciation of the Greenland and Laurentide ice sheets interrupted by glacier advance during abrupt coolings. Quat Sci Rev 229. https://doi.org/10.1016/j.quascirev.2019.106091.